Recurring Slope Lineae on the Northern Hemisphere of Mars: an investigation into new candidate sites

Andreas Eriksson

Degree of Master of Science (120 credits)
with a major in Earth Sciences
45 hec

Department of Earth Sciences
University of Gothenburg
2018 B1010

Faculty of Science

UNIVERSITY OF GOTHENBURG

UNIVERSITY OF GOTHENBURG
Department of Earth Sciences
Geovetarcentrum/Earth Science Centre

Recurring Slope Lineae on the Northern Hemisphere of Mars: an investigation into new candidate sites

Andreas Eriksson

ISSN 1400-3821

B1010
Master of Science (120 credits) thesis
Göteborg 2018

Mailing address
Geovetarcentrum
S 405 30 Göteborg

Address
Geovetarcentrum
Guldhedsgatan 5A

Telephone
031-786 19 56

Geovetarcentrum
Göteborg University
S-405 30 Göteborg
SWEDEN

Abstract

Recurring Slope Lineae (RSL), are dark markings found on slopes with a steepness of 25°-45°. Their width is between 0.5-5 m but they can become hundreds of meters long. They grow incrementally during warm seasons; fade during cold seasons and appear again the following Mars year. They occur mainly in the equatorial and southern mid-latitudes and appear less abundant in the northern hemisphere. After the first confirmed observations of RSL, research about them accelerated quickly. This is mainly because of their possible origin as water flows at the modern day martian surface. The main scope of this thesis is to find new RSL candidate sites in the less investigated northern hemisphere. Furthermore, the thesis investigates if potential candidate sites are wet- or dry flows since the processes behind RSL are still debated. By using a GIS ArcMap model, data from the High Resolution Imaging Science Experiment (HiRISE) instrument and parameters based on previous literature, new optimal sites for RSL were found with 27 of those areas having features being classified as new candidate RSL. Analyses of interesting candidate sites with modelled temperature measurements, grain size approximations, modelled water vapour data and parameters derived from previous studies suggests that a combination of wet flows and dry flows may be responsible for the creation of RSL. The reason for the scarcity in the northern region is due to less favourable RSL forming areas, less HiRISE coverage and less favourable temperature parameters on the northern hemisphere. For future studies it is suggested that more HiRISE images are gathered for the candidate sites and more research is done on a combined model of RSL creation.

Keywords: Recurring Slope Lineae, RSL, Mars, HiRISE, Candidate sites, GIS, Northern hemisphere.

Sammanfattning

”Recurring Slope Lineae” (RSL) är mörka markeringar på sluttningar med en lutning på 25°-45°. Bredden ligger på 0.5-5 m men de kan bli flera hundra meter långa. De växer sig stegvis längre under varmare säsonger och bleknar under kallare säsonger och dyker upp igen under följande Mars år. De förekommer runt ekvatorn och på den södra hemisfärens mellan latituder men inte på den norra hemisfären. Efter att man bekräftat den första observationen av RSL så accelererade forskningen om dem. Detta beror troligtvis på dess möjliga ursprung som vattenflöden på ytan av nutidens mars. Huvudmålet med den här studien är att hitta nya kandidatplatser för RSL i den mindre utforskade norra hemisfären. Studien utforskar även om RSL vid de potentiella kandidatplatserna är vattenflöden eller torra flöden då processerna bakom RSL fortfarande är debatterade. Genom att använda en GIS ArcMap modell, bilder från ”High Resolution Imaging Science Experiment” (HiRISE) instrumentet och parametrar baserade på tidigare studier, hittades många nya optimala platser för RSL där 27 stycken klassificerades som kandidater. De mest intressanta kandidatplatserna analyserades med modellerad temperaturdata, kornstorleksapproximationer, modellerad data av vattenånga och parametrar från tidigare studier. Genom detta föreslås en kombination av vattenflöden och torra flöden vara den process som skapar RSL. Anledningen till att de är sällsynta i den norra hemisfären är på grund av mindre antal möjliga platser för RSL att skapas på (branta backar etc), mindre täckning av HiRISE bilder och mindre bra temperatur parametrar på norra hemisfären. För framtida studier föreslås att mer HiRISE bilder samlas för kandidatplatserna och att mer forskning kring den kombinerade modellen för RSL blir gjord.

Nyckelord: Recurring Slope Lineae, RSL, Mars, HiRISE, Kandidatplatser, GIS, Norra hemisfären.

Table of Contents

1. Introduction

Due to several successful planetary missions in the last two decades our understanding about Mars has increased significantly. In this relatively short period of time, both orbital and lander missions have contributed to ground-breaking discoveries about past and current environments, climate, landforms and processes on modern-day Mars. Today, one of the most intense scientific endeavours is to get a better understanding of the currently active surface processes and how they shape the martian landscapes. This scientific inquiry of change detection was made into a possibility due to the development of powerful orbital instrumentation that allows repeat observations of small-scale landforms and surface features on Mars over multiple seasons or years. Repeat observations during the last decade have altered our view of Mars in profound ways from being a geologically dead planet to a currently dynamic planet where CO_2, wind, ice and potentially water play active roles. However, there are still many unknowns and new discoveries are made every day. One of these discoveries is Recurring Slope Lineae (RSL) that was first described by McEwen et al. (2011).

RSL's are small to narrow dark markings ranging from 0.5 to 5 meter in width and can become several hundreds of meters long (Figure 1). They mostly appear on equator-facing 25°-40° degree slopes but can occur on slopes facing other directions as well. One of their most prominent features is their reappearance at the same locations over multiple martian years, where one martian year is approximately two Earth years. RSL incrementally grow during the warmer spring to summer season and fade during the colder autumn and winter seasons until it disappears. RSL then appear once again during the spring season (McEwen et al., 2011). The temperature range at which RSL are active is considered to be 250 K-300 K (Kelvin) where 273.15 K is equal to 0°C. RSL also have a tendency to develop in areas with an albedo value <0.2 (Ojha et al., 2015).

The aim of this study is to investigate the northern hemisphere to see if there is a potential for more RSL sites in that region. Possible candidate RSL sites will be analysed in order to answer two additional research questions. Firstly, why are there less RSL's in the northern hemisphere than in the mid latitudes and southern hemisphere? The second research question is about the processes that is generating RSL. It is uncertain how they are formed and what is the true driving force behind them. The purpose of these questions, especially the second one, is to get a better understanding of RSL since there are still major uncertainties about them. Currently two main formative hypotheses for RSL are prominent; that they are

either created by granular flows (dry flows) or through some forms of wet flows (Dundas et al., 2017; McEwen et al., 2011). By analysing possible candidate RSL location(s), this thesis aims to find evidence that support either hypotheses in order to better determine the most likely formative mechanism for RSL at the candidate sites.

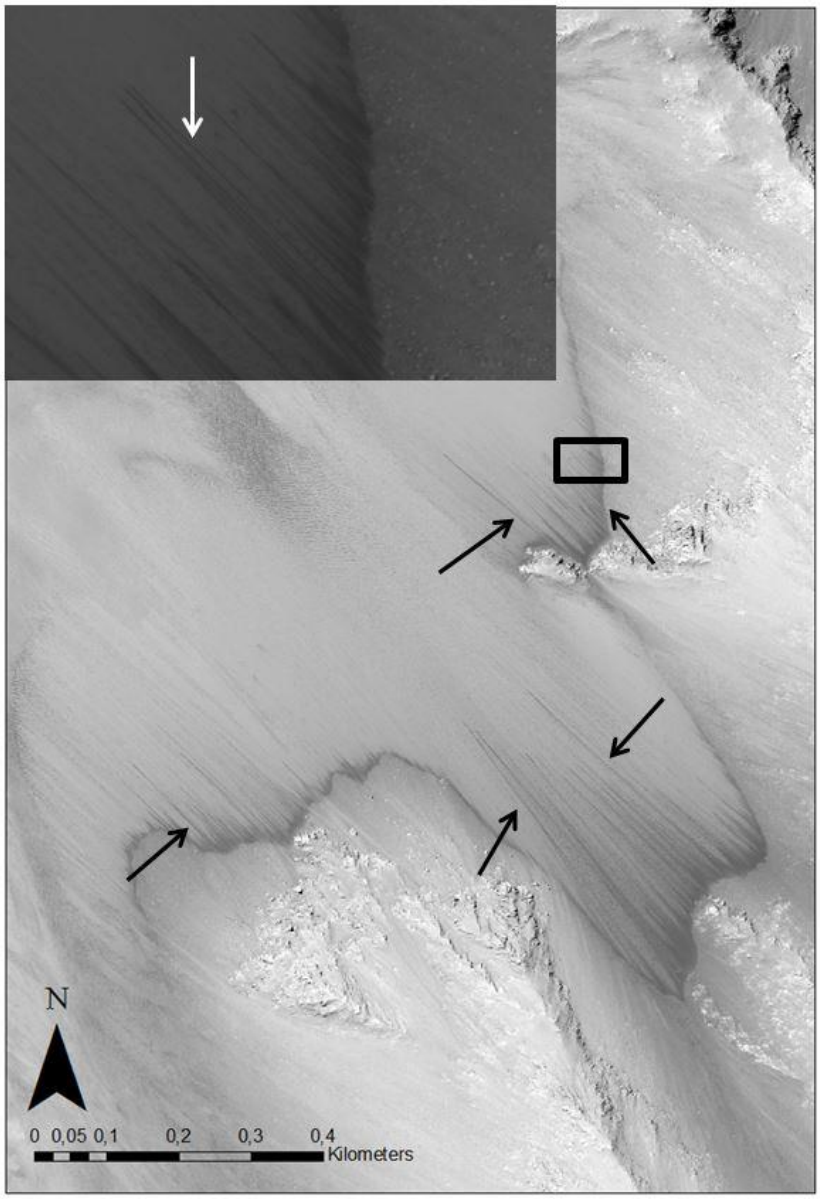

Figure 1: Example of RSL from image ESP_034830_1670. Long dark lineae pointing in a NW direction is supposed to be RSL. Solar Incidence angle is 60°, with the Sun about 30° above the horizon. Image taken from the HiRISE instrument and the Mars orbital data explorer (W.U, 2018). Credit: NASA/JPL/University of Arizona

1.1 Study Area

This thesis will cover most parts of the northern hemisphere in order to be sure that interesting areas will be within the parameters of the analysis. The area include the entire longitudinal extent from 0° to 360° and an latitudinal extent which reaches from the 30° latitude to the 90° latitude (Figure 2). The only area not included within these parameters is Acidalia Planitia and

parts of Chryse Planitia. This is because there already are RSL's within those areas and this study want to find new areas with RSL and not focus on already detected RSL.

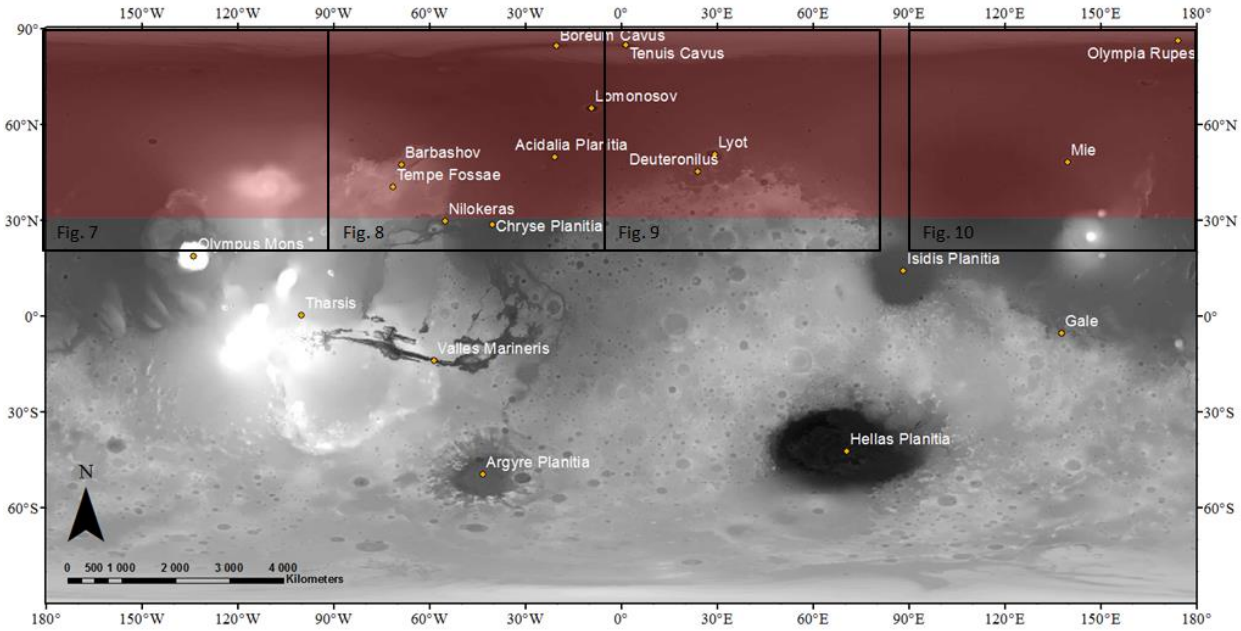

Figure 2: Overview map of Mars with labels of frequently mentioned areas on the Martian surface. The light red color shaded area represents the study area that is above the 30th latitude. The black boxes are inset images showing the location of figures 7-10 found in 3.1. Cartographer was Andreas Eriksson. Basemap is a Thermal Emission Spectrometer (TES) image from Christensen et al. (2001) and U.S.G.S. (2014).

1.2 Background

Multiple orbiters, landers and rovers have obtained data about Mars with varying success since the Mariner mission in the late 1960's. A reason for this thirst of knowledge is the long standing idea of water on Mars and the possibility for past or extant life. Over the course of several decades, data and images have led to remarkable discoveries of the surface geology and climate of the red planet. However, RSL's were detected only recently because of the advent of high-resolution imaging that is capable at resolving such small-scale features.

When the Mars Reconnaissance Orbiter (MRO) satellite was launched on the 12th of August 2005 it had several new instruments equipped. One of these was the High Resolution Imaging Sciences Experiment (HiRISE) with an image resolution down to 25 cm/pixel. It can easily detect objects of 1 meter in size on the martian surface. The satellite got into orbit on the 10th of March 2006 and started acquiring images in November the same year (McEwen et al., 2007). It has since then recorded a multitude of images covering ~4% of the martian surface and will continue recording images until at least 2025. One powerful aspect of the HiRISE instrument is the ability for researchers to acquire repeat-coverage of small-scale landforms and possible change detection. From this new high resolution database McEwen et al. (2011) and others discovered and further mapped the new RSL phenomena (McEwen et

al., 2013; Ojha et al., 2014; Stillman et al., 2016; Stillman, Michaels, Grimm, & Harrison, 2014).

As RSL was recognized and first properly analysed, they were mostly found in the equatorial and mid-latitude regions of Mars (McEwen et al., 2011). The many aspects of RSL, such as seasonality, led researchers to hypothesize that RSL had some sort of water source where shallow aquifer release, deliquescence from atmospheric water vapour or brine flows were possible scenarios. The salts associated to brine flows can potentially lower the freezing temperature of water by 70 K. With a new possibility of water, the interest for RSL grow (McEwen et al., 2007; McEwen et al., 2011; Ojha et al., 2014; Ojha et al., 2015; Ojha et al., 2013; Stillman et al., 2014).

One of the current, reasonable hypotheses is the one focusing on brines and brine flows. During a warm season, temperature will rise in the subsurface. This will cause percolation downslope because we have an interface of a frozen brine layer as well as liquid brine (McEwen et al., 2011). The water needed for the brine can come from several sources. One is from deliquescence where salt sources on the martian surface absorb water vapour from the atmosphere. The other is water from a potential groundwater source or ice in the regolith (McEwen et al., 2011).

With an increased interest, mainly due to RSL being a potential water source, even more areas of RSL were discovered with a preference towards the southern hemisphere (McEwen et al., 2013; Ojha et al., 2014). However, fewer sites were identified on the northern hemisphere. As of now, a majority of RSL sightings occur on the southern hemisphere with fewer identified RSL on the northern hemisphere. The scarcity of RSL in the northern hemisphere is not fully understood and has yet to be explained (Ojha et al., 2014). In the northern hemisphere, the most prominent RSL site is situated in Acidalia- and Chryse planitia. This one site is a confirmed RSL site among the few that is found in the northern hemisphere (McEwen et al., 2013).

According to some studies RSL is unique to Mars (Ojha et al., 2014). However, a potential terrestrial analogue for RSL may be something known as ‘water track’. They are basically areas of higher soil moisture content than the surrounding slope that can lead shallow surface conduits where saline water progresses down a slope. This mostly occurs above the permafrost a few centimetres subsurface. ’Water tracks’ can go through the surface via fine-grained materials on lower slopes which can create lineae on the surface that can darken in a seasonal way. The location where this feature is most discussed is in Don Juan Pond (DJP) located in Antarctica (Dickson, Head, Levy, & Marchant, 2013; Levy, 2012).

In recent years the thought process concerning the source for RSL is under review. These thought processes suggests that water only has a small part to play in the creation of RSL and that a granular flow is a more plausible idea. The reason for the new 'dry flow' way of thinking was new observations regarding RSL. One observation was concerning the "angle of repose" where terminal slopes of lineae matched the angle where cohesionless sand stops. Dundas et al. (2017) observed recurring slope lineae in Eos Chasma and found that these matched the angle of repose. He further observed that the length of the lineaes differed a lot where the longer lineae where those that best corresponded with the angle of repose. This was not consistent with water models and was then thought to be more like a granular flow (Dundas et al., 2017). The recharge feature for the granular flows is believed to be similar to climbing dunes. Material advances up the slope and adds more sand to slope, in a potential aeolian type feature. Another observation or idea explained the darkening of RSL as "particle size and roughness effects". Both hypothesis, describing a water source or a dry source cannot fully explain all aspects of RSL and need further research (Dundas et al., 2017).

1.3 Brief Geologic History of Mars

Mars has, just as Earth, gone through many changes since its formation about 4.5 Ga years ago. As Mars was formed, it is believed that it created the crust, mantle and core within only several million years after our solar system was formed. Isotope data of tungsten and neodymium (^{182}W and ^{142}Nd) from meteorites as well as meteorites from 4.5 Ga indicate this (Carr & Head, 2010). The earliest stage known as pre-Noachian is characterized by a magnetic field and basin forming impacts where one such impact may be the cause for the global dichotomy that basically created two distinct parts of Mars (Carr & Head, 2010). The global dichotomy is characterized by distinct differences in elevation and crustal thickness. The difference in elevation between the northern and southern part of the dichotomy is 5.5 km. The crustal thickness varies but is approximately 30 km in the northern hemisphere and 60 km in the southern hemisphere. How it was created is currently unknown (Carr & Head, 2010; Mangold, Baratoux, Witasse, Encrenaz, & Sotin, 2016). It is possible to make the observation that the pre-Noachian corresponds to the Hadean period on Earth since it is hard to obtain information from this era (Mangold et al., 2016).

The pre-Noachian ranges from the formation of Mars too around 4.1 Ga (Figure 3). This is based on the formation of Hellas Planitia which is the starting point for the Noachian period. It ranges from 4.1 to approximately 3.7 Ga.

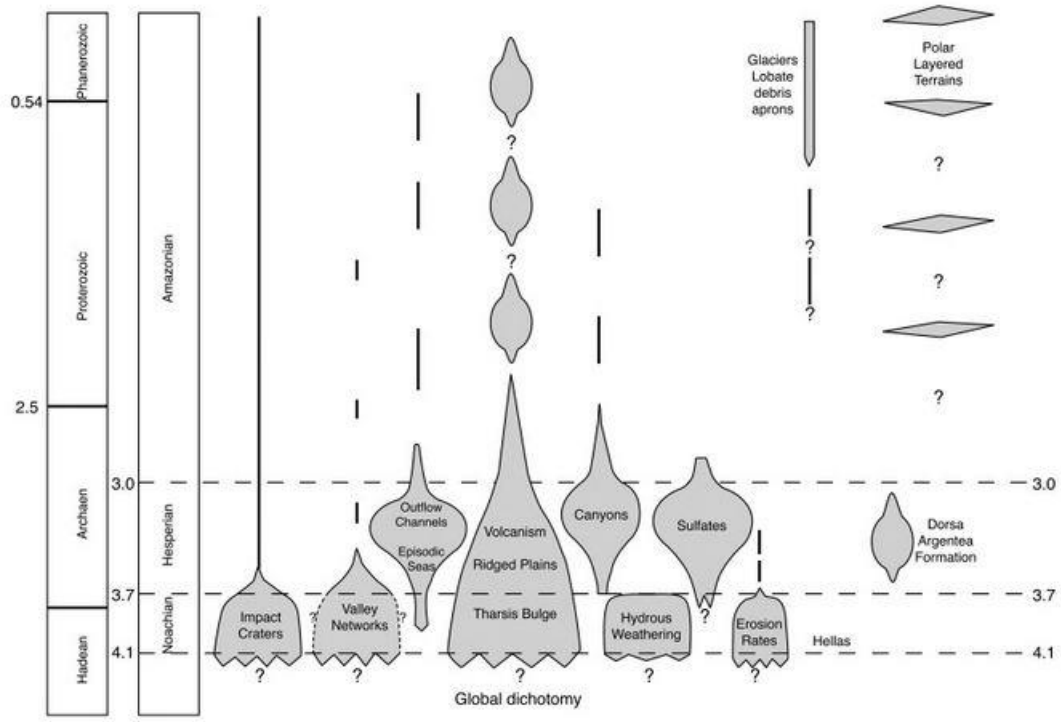

Figure 3: Image show major geological activities on Mars based on time. The important part is the time scales to the right. On the far right we have Earths time periods in correlation with Mars different time periods on the left of it. Image taken from Carr and Head (2010).

Continued formation of impact craters happened in the Noachian. Many craters larger than 100 km can be spotted from this era. Other prominent features of the Noachian impact craters are erosion and weathering. Noachian craters have heavily weathered and eroded rims as well as a significant amount of crater infill. The terrain in general is much more eroded and weathered than terrains from younger periods. A side effect of the weathering is that phyllosilicates can be found in regions dating to this period. The phyllosilicates along with geomorphological evidence may suggest that liquid water was available during this period. Geomorphological evidence include extensive dendritic features on valley networks, fluvial deltas and paleo lakes that was found to be from this period (Carr & Head, 2010).

Volcanism was another important feature of the Noachian period. One of Mars major volcanic provinces "Tharsis" (close to Olympus mons) was formed (Carr & Head, 2010; Mangold et al., 2016). There are two more time periods that defines Mars (Figure 3). These are the Hesperian and the Amazonian (Carr & Head, 2010).

The Hesperian period starts around 3.7 Ga by the end of the late heavy bombardment and reaches to the 3.0 Ga point. This time period is said to have widespread volcanism that created lava plains over large areas. Compared to the Noachian period there is much lower rates of erosion and valley formation. The creation of phyllosilicates dropped substantially to almost stop completely. However, this period sees formation of many other geological

features; canyons such as Valles Marineris were formed in this time period, there was a large build-up of deposits containing abundant sulphates and seas and terminal lakes were potentially formed. This means that bodies of liquid water with shorelines have potentially been present in areas such as the northern hemisphere (Carr & Head, 2010).

The last geologic time period of Mars is known as the Amazonian. It stretches from 3.0 Ga to the present day. This period is distinctively known for aeolian and ice-related activity and the build-up of the polar ice caps that probably helped shape the geomorphology of Mars through time. An abundance of ice is found in Polar Regions and in the mid-latitudes. Ice and wind are the main processes that has changed and altered the terrain in this time period, much more so than in previous time periods. However, a similar pace of erosion and weathering as the Hesperian is found in the Amazonian. Cyclical changes in obliquity have affected processes throughout Mars history but in this time period these changes are more apparent. Other prominent processes such as impacts and volcanism is not as frequent and is not the main contributor to the surface processes but still effects certain areas more than others such as Tharsis (Carr & Head, 2010; Mangold et al., 2016).

1.3.1 Minerology and Landforms

A major component of the surface is tholeiitic basalts enriched in Fe with olivine, pyroxene and feldspar as its component. There is also granitoids that have a high content of felsic and alkali components. They come in the form of granodiorites and can be found on conglomerate clasts (Mangold et al., 2016). As previously stated phyllosilicates (clay minerals) can be found on Mars surface. Some examples of the minerals are montmorillonite and Fe-rich chlorites. Another main type of minerals found on Mars is sulphates (see 1.3) where one example is gypsum. Other types of minor minerals that can be identified on Mars are for example carbonates (Carr & Head, 2010; Mangold et al., 2016).

Dunes are abundant on Mars. They can be in a larger class and have darker tones due to basaltic sediments or be smaller in the form of aeolian made ripples. The most common areas to find dunes in are around the northern and southern polar cap where they form large ergs (sand seas). Wind-blown sediments are also trapped inside impact craters and dunes are common landforms on many crater floors. The most common types of dunes are Barchan dunes and longitudinal dunes (Mangold et al., 2016).

Dust devils may not be a landform but rather a common surface process on Mars that leave bright or dark surface tracks along their paths. They are created through thermal convection when the ground heats up. This is very similar, if not the same, as on Earth,

although they grow much larger in size and contribute significantly to the overall dust budget of the martian atmosphere. Another larger transport of dust is dust storms that can become planet-wide on Mars. They are seasonal and the dust in both the storms and the dust devils has a basaltic composition with iron oxides that are about 1 μm (Mangold et al., 2016).

Gullies are degrading-aggrading landforms, featuring an alcove of source materials with a channel leading into a depositional fan. They are most abundant in the mid-latitudes with a few exceptions in the equatorial areas. They occur on interior crater walls, hillslopes and valley walls (Harrison, Osinski, Tornabene, & Jones, 2015; Malin & Edgett, 2000). They are possibly connected with water related processes (Johnsson, Reiss, Hauber, Hiesinger, & Zanetti, 2014), although dry processes triggered by CO_2 has recently been proposed (M. Dundas et al., 2017).

There are many different types of large-scale channels found on Mars. Valley networks and outflow channels are thought to be fluvial processes. Valley networks are believed to have formed during a time in early Mars history when it had thicker and warmer atmosphere. This climate would have supported liquid standing bodies of water at the surface for a long period of time. The valley networks probably formed due to precipitation, runoff and fluvial erosion forming dendritic valley systems.

Evidence for remnant deltas associated with valley networks on Mars adds further evidence for prolonged water activity in earlier periods of Mars. The delta fans are larger in extent in Noachian time than in following periods and the older deltas have a bigger volume than those created later. The latter go up to a few km^3 in volume and the older will be at least twice that size (Mangold et al., 2016).

In contrast, the onsets of large outflow channels came later and are considered independent of climate since they formed during a time when the surface was to cold and the atmosphere too thin to support liquid surface water. The outflow channels are proposed to have formed due to breaching of a confining cryosphere where groundwater under artesian pressure could escape to the surface. As such outflow channels were indicated to be catastrophic floods that occurred in pulses during the Hesperian period and declining onwards. The breach of the cryosphere may be due to impacts, volcanism or tectonics. Temporary lakes may have formed because of the escaped water that froze and sublimed over time. One of these outflow channels can be found in Chryse Planitia (Mangold et al., 2016).

These are only a few landforms and features. Since the martian surface represent a multitude of landscapes that formed at different times and varying conditions a more comprehensive description will be too exhaustive within the scope of this thesis.

1.3.2 Water on Mars

As presented in the above sections, liquid water has likely played a key role on Mars in the distant past, although the initial quantity and fate of the water are still not fully understood (McEwen et al., 2007). In earlier years scientists have debated the possibility of an early ocean in the northern hemisphere on Mars. The first hypothesis built on the observations of putative preserved ancient shorelines (Parker, Gorsline, Saunders, Pieri, & Schneeberger, 1993). They are, however, questioned because they are not fully supported by topographic results or by high resolution interpretations (Mangold et al., 2016). It is also possible that they are volcanic contacts (Carr & Head, 2010). Geomorphologic evidence points both ways where some argue that many Noachian features cannot be seen any more and others claim evidence still proves the existence of a paleo-lake in the past (McEwen et al., 2007). In recent years the ocean-hypothesis has gained some support by observations of what may be ancient tsunami resurfaced plains (Costard et al., 2017; Rodriguez et al., 2016).

With findings of outflow channels it is suggested that liquid bodies of groundwater may remain in the deep subsurface (Carr & Head, 2010; Mangold et al., 2016; McEwen et al., 2007).

Past water in the northern plains is also suggested by the presence of clay minerals found at depth in craters and sediments transported by potential floods in buried ridges. Stagnant ice left behind in these areas is features that can point to water bodies (Carr & Head, 2010; Mangold et al., 2016). One problem with these theories are an apparent lack of evaporites (Carr & Head, 2010).

Ice is an important aspect in the question about the fate of the water. Ice is mostly found on the polar caps but can be found in the mid latitudes as well (Mangold et al., 2016). This is mostly dependent on seasonal activity but also on obliquity. In relatively recent times on Mars, high obliquity excursions of more than 30° resulted in more water in the atmosphere due to polar warming. The water got redistributed towards the mid-latitudes that now acted like a cold sink (Head, Mustard, Kreslavsky, Milliken, & Marchant, 2003). These periods are called ice ages on Mars (Head et al., 2003). Currently, Mars is in an interglacial period where the obliquity is stable around 25° and ice in the low mid-latitudes are now escaping towards the poles (Forget, 2007; Head et al., 2003; Mustard, Cooper, & Rifkin, 2001). The currently known water inventory from the observable frozen reservoirs corresponds to a global martian ocean of 34 m depth (Carr & Head, 2015).

2. Data and Methods

In order to work with the available data sets several types of software's were used. The Mars Climate Database (MCD) was used in order to get temperature data for an analytic model in the first part of the thesis. The MCD is a database that provides information of the martian climate. The MCD uses a General Circulation Model (GCM) that provides calculated simulations of Mars atmosphere. The simulations were certified with 'available observational data' (Forget et al., 1999; Millour et al., 2015). The resolution of the MCD can get down to 32 pixels per degree when interpolating to high resolution topography (Forget et al., 1999; Millour et al., 2015).

MCD provided "average max mean daily temperature" for the analytical model. The same parameter was used in phase three of the thesis (see 2.3) (Forget et al., 1999; Millour et al., 2015). In the MCD it was possible to change settings for the parameters. The settings were for example 'time of day', Solar Longitude (L_s) and 'altitude'. The altitude setting was set to 'near surface' which is equal to 2 meter above the surface. Most of the HiRISE images used in the study are taken in the afternoon by the instrument. This forced the 'time of day' setting to be set at a local time of Martian hour 15. The solar longitude was set to be during the northern summer season (110 L_s) in order to meet the utmost conditions for RSL. L_s are described as a measure of martian seasons. Data set coordinates were all set to match the extent of the study area (Forget et al., 1999; Millour et al., 2015).

Data processing for the first phase and for interesting RSL images in phase 3 were done in the Geographical Information System (GIS) ArcMap. All data coordinates from MCD used the "Inverse Distance Weighted" (IDW) Interpolation spatial analyst tool to display data on the GIS maps. The interpolation tool interprets values closer to each other to be more similar than those further away. To obtain a value in an area where there is none, the tool uses measured values in close proximity to the unmeasured area to get a good prediction of a potential value. Values closer to an unmeasured site have a higher impact on the result than values further away. Distances to values are very important in this interpolation tool (Philip & Watson, 1982; Watson & Philip, 1985).

For image review the software HiView was used. This accessory software is used in connection with HiRISE images. The high resolution of the images can be properly viewed and thoroughly investigated in this software (Castalia, 2012).

All of the laboratory work on this thesis, including the GIS work and other software, was conducted at Geovetarcentrum, the Department of Earth Sciences and University of Gothenburg.

2.1 Phase 1: Establishing potential areas

The study area is the vast northern hemisphere of Mars as explained in 1.1 and Figure 2. To search for RSL over the entire surface is difficult and time consuming. It is far better to look into specific areas of interest instead. Because of this an analytical model is used based on parameters found in several academic reports (McEwen et al., 2013; McEwen et al., 2011; Ojha et al., 2014). This produces a map with a smaller amount of optimal sites which is looked into further.

Data processing for an analytical model is conducted in ArcMap and based on the following conditions: Slope angle degree of 25°-40°, thermal inertia of about 200-340 J m^{-2} $s^{-1/2}$ K^{-1}, albedo <0.2 and a temperature range of 250-300 K. Basemaps from the U.S.G.S. (2014) were used as the framework for the analyses. They use the 'Mars2000_ECylindrical_clon0' or the 'Mars2000_Simp_sphere_clon0' as coordinate systems for the basemaps (Forget et al., 1999; McEwen et al., 2013; McEwen et al., 2011; Millour et al., 2015; Ojha et al., 2014; U.S.G.S., 2014). The coordinate system for the HiRISE images is set as 'Equirectangular_Mars' (W.U, 2018). The mentioned conditions are used because RSL are most likely occurring within the range of those parameters (McEwen et al., 2011).

An important note to mention is the slope angle degree parameter and the uncertainty of the slope data. This thesis uses Mars Orbiter Laser Altimeter (MOLA) as topography and elevation data. The benefit of MOLA is that it is easily accessible and covers the whole study area, but it is insufficient to resolve the actual slope values for small-scale features such as RSL. Nevertheless, it is suitable for locating available slopes over vast areas. The MOLA data was transferred into the ArcMap software for further processing. The 'slope tool' from the 'Spatial Analyst Tools', in the 'ArcToolbox' was used to create the slope data from MOLA. This is not the most accurate instrument and may not have the accuracy to exactly pinpoint slopes of 25°-40°. However, this thesis would mostly like to find sufficient slope terrain or leaning terrain in which there might be RSL. For this reason MOLA is used and the slope angle degree is set as 25°-40° which could vary slightly in the model due to accuracy reasons. Another reason is that it was easy to use and implement into the model.

MOLA is a remote sensing instrument aboard the Mars Global Surveyor (MGS). The spacecraft was on the 7 of November in 1996 and MOLA transmitted data till at least 2001. The instrument measured distances between MGS and the martian surface using laser pulses in order to acquire topography data and obtain better elevation data on the martian surface. One important goal was to "map globally the topography of Mars at a level suitable for

geophysical, geological and atmospheric circulation studies of Mars" (Smith et al., 2001). The resolution for the MOLA datasets are 1/64° in latitude times 1/32° in longitude with 1 X 2 km^2 at the equator (Smith et al., 2001). This is the resolution of MOLA's topographic grid.

The model is created in the "model builder" tool in the ArcMap software (Figure 4). All the parameters were implemented into model builder and reclassified by the 'Reclass' tool to find the proper classes for each parameter. They were linked to the weighted overlay where the different conditions were weighed depending on their importance. The following percentages set in the weighted overlay are based on assumptions made by this thesis. This was done in order to put emphasis on what this thesis believes is the most important aspects of the model. The slope was set to 60% as this is one of the more important aspects for RSL. Temperature was set to 20% as it is less important than the slope but more important than the remaining criteria as a controlling factor. The thermal inertia and albedo was both set to 10% as they were thought to have the lowest importance in finding suitable sites for this model.

The accuracy of the model was tested by applying it on the southern hemisphere using the same parameters as on the northern hemisphere. As a reference, confirmed sites from McEwen et al. (2013) was used as a comparison in order to see if they were in close spatial proximity to the optimal sites found on the southern hemisphere (see 4.1.2).

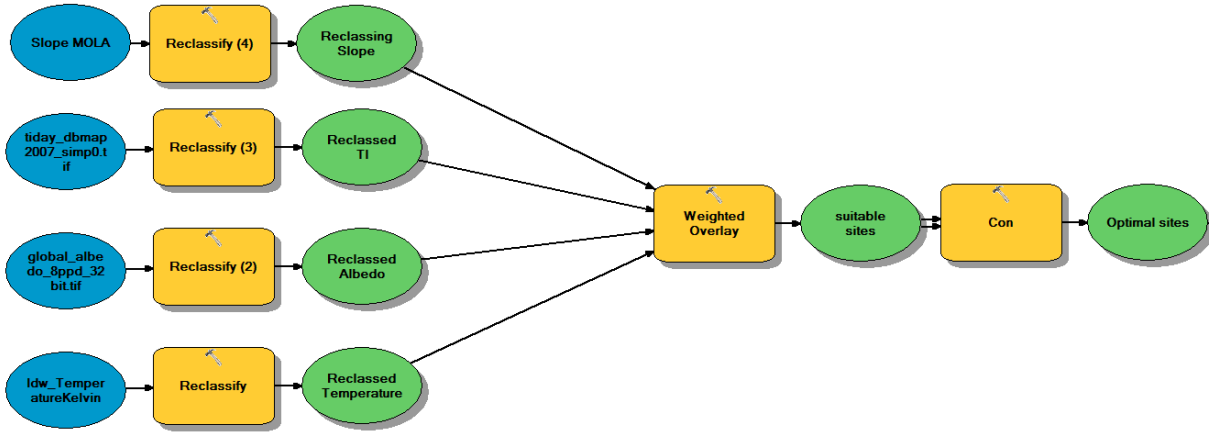

Figure 4: The model that was created in the model builder tool from the GIS software ArcMap. From top to bottom in the blue ellipses are the slope data, Thermal inertia, Albedo and Temperature data. All were reclassified and run in a weighted overlay. A condition value was set in order to find the most optimal sites from the suitable sites.

2.2 Phase 2: Confirming RSL candidate sites

With the help of the analytical model, it was possible to find images taken by the HiRISE instrument. HiRISE has a max resolution of 25 cm/pixel and was used for the analyses in phase 2 (Figure 5a) (McEwen et al., 2007).

The HiRISE instrument can obtain images with 28 Gb of data in about 6 seconds. During a two year Primary Science Phase (PSP) the instrument has returned roughly 12 Tb of

data. HiRISE uses several different components to obtain the images. One of the components that acquire the images is known as a Charge-Coupled Device (CCD). HiRISE is equipped with 14 CCDs. There are different types of CCDs depending on colour filters, being red, blue-green and near-infrared. The three filters create false colour images. This means HiRISE create images in a spectrum outside of the visual spectrum (VIS). This makes it possible to analyse the images for different materials and specific textures (McEwen et al., 2007).

Through the "Mars orbital data explorer" (W.U, 2018) database, orthorectified HiRISE images within and in close proximity to the optimal sites found in phase 1 were collected for further study. A HiRISE image provides several other image types over one and the same area which means that multiple types of each HiRISE image were analysed. A "black and white" image type and a "colour" image type were examined for each HiRISE image. In order to be extra thorough, merged images for the two mentioned types of images were looked at as well. This means that this thesis has looked at multiple images over the same area which have added to the number of images looked at. However, technically there are only approximately half the amount of sites looked at because of this. Other landforms such as mesas and dunes where documented for further studies.

After a first round of analyses, sorting and looking through images found in the Mars orbital data explorer that was based on the optimal sites from phase 1, the images with potential RSL content and interesting features corresponding to other academic works such as McEwen et al. (2011) and Ojha et al. (2014) went through a second round of analyses. In this stage, the images were evaluated with the software HiView (Castalia, 2012). Each potential RSL was divided into a specific class (as described below) to determine the type of RSL that was found. Criteria for each class are based on academic works by Ojha and Stillman (Ojha et al., 2014; Stillman et al., 2016). The "candidate" class is basically an RSL like feature where no recurrence or incremental growth was detected. It is simply a lineae which requires further investigation. The "partially confirmed" class has either recurrence or incremental growth but not both are observed. The geologic and environmental setting is correct but insufficient data stops it from being the "confirmed class". This class has both recurrences over several Mars years, an incremental growth that fades during the winter season and all settings such as albedo and slope degree are accurate. Images that were not designated to any of these classes were set as a non RSL site (Ojha et al., 2014). A Venn diagram (Figure 5b) was used to complement the previously mentioned criteria (Stillman et al., 2016).

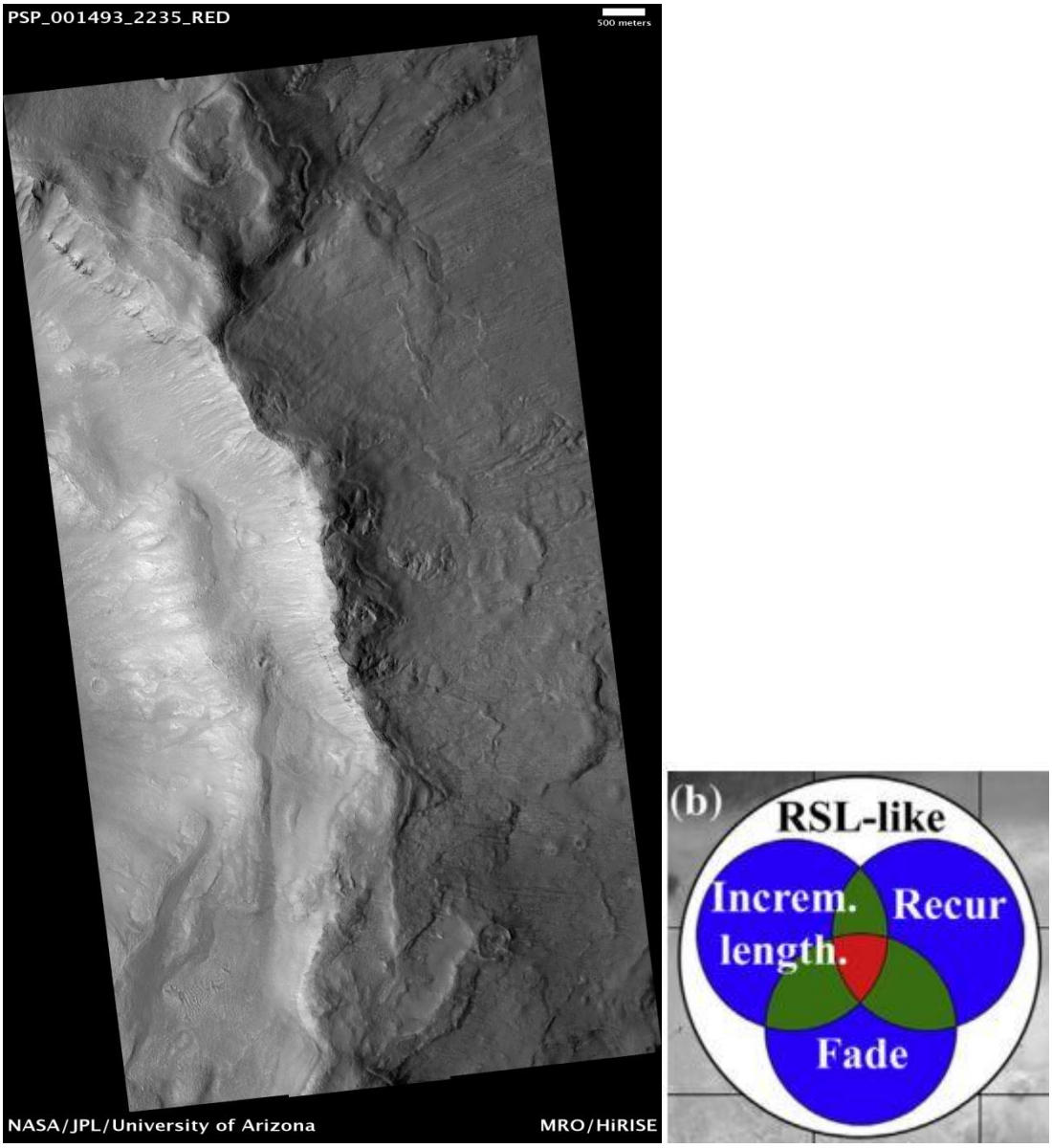

Figure 5: The first image a) is an example image from the HiRISE instrument. The image is the standard site PSP_001493_2235 (I) that is used in this thesis. Solar incidence angle is 50°, with the Sun about 40° above the horizon. Credit: NASA/JPL/University of Arizona. b) A Venn diagram taken from Stillman, Michaels, Grimm, and Hanley (2016). It was used in determining the classification of RSL.

2.3 Phase 3: In depth investigation

The two major ideas about the formation and sources of RSL, the dry (granular) flow versus the wet flow will be tested based on images from this thesis (Dundas et al., 2017; McEwen et al., 2011). Some of the most prominent potential RSL locations from phase 2 will be used for the analysis.

Water vapour (H_2O) column, CO_2 column and temperature data was collected from MCD to discuss potential deliquescence, seasonal frost and temperature dependent processes (Forget et al., 1999; Millour et al., 2015). This data was handled in the ArcMap software. The

parameters for MCD was set as for phase 1 except for the altitude setting which now could be set to 0 meters above ground.

From the high resolution images different surface features and landforms were identified. Alcoves and the terrestrial analogy for RSL, 'water tracks', were looked for specifically in order to see similarities between images and other literature. Using thermal inertia a potential grain size was measured for each image. Thermal Inertia is a measure of the rate at which an object loses heat or gain heat to its surroundings. It is used to find grain sizes because it is connected to "the particle size of unconsolidated deposits at martian atmospheric pressures" (Edgett & Christensen, 1991). A graph (Edgett & Christensen, 1991) was used as a reference for this (Figure 6). Salt data from the Compact Reconnaissance Imaging Spectrometer for Mars (CRISM) aboard the MRO could not be used due to time constraints.

By comparing these parameters to other literature (Dickson et al., 2013; Dundas et al., 2017; Edwards & Piqueux, 2016; McEwen et al., 2013; McEwen et al., 2011) a hypothesis will be formulated. The hypothesis will tell if the potential RSL is thought to be a dry flow or a wet flow.

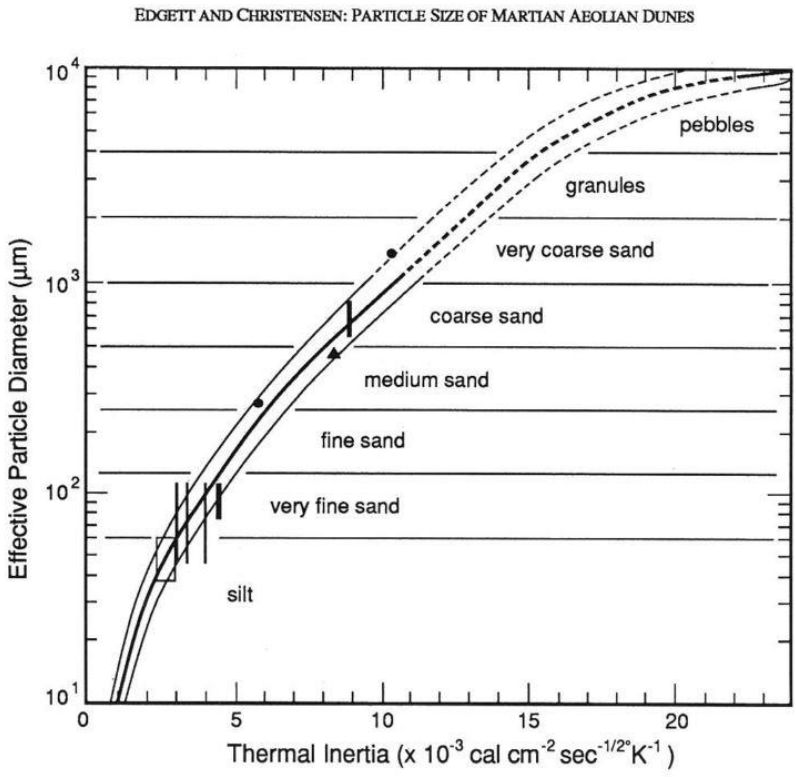

Figure 6: Grain size graph based on thermal inertia that was used to obtain hypothetical grain sizes for candidate RSL's in phase 3. Graph is taken from Edgett and Christensen (1991).

3. Results

3.1 Phase 1

The outcome shows 331 pixels equal the parameters set by the ArcMap model (Figure 7, Figure 8, Figure 9 & Figure 10). The total amount of pixels in the model is 132638 with a pixel size of 7409X7409. This gives us an area of ~0.3% that was hit by the model. However, 53 pixels are within Acidalia Planitia and Chryse Planitia which is not looked at in this thesis. This means that 278 optimal sites including their surrounding areas will be the baseline for phase two.

The sites are widespread across the northern hemisphere with a much denser number of sites closer to the mid latitudes at the bottom end of the red area in Figure 8 & Figure 9. The densest populations are found under the Lyot crater (around Deuteronilus Mensae), left of Chryse Planitia around Nilokeras, right of Chryse Planitia and around Barabashov crater above Tempe Fossae (Figure 2). This follows studies of McEwen et al. (2013) who also investigated areas close to the northern mid-latitude.

In the northern plains, most sites are spread out over all longitudes and are mostly only found in craters such as Lomonosov or Mie.

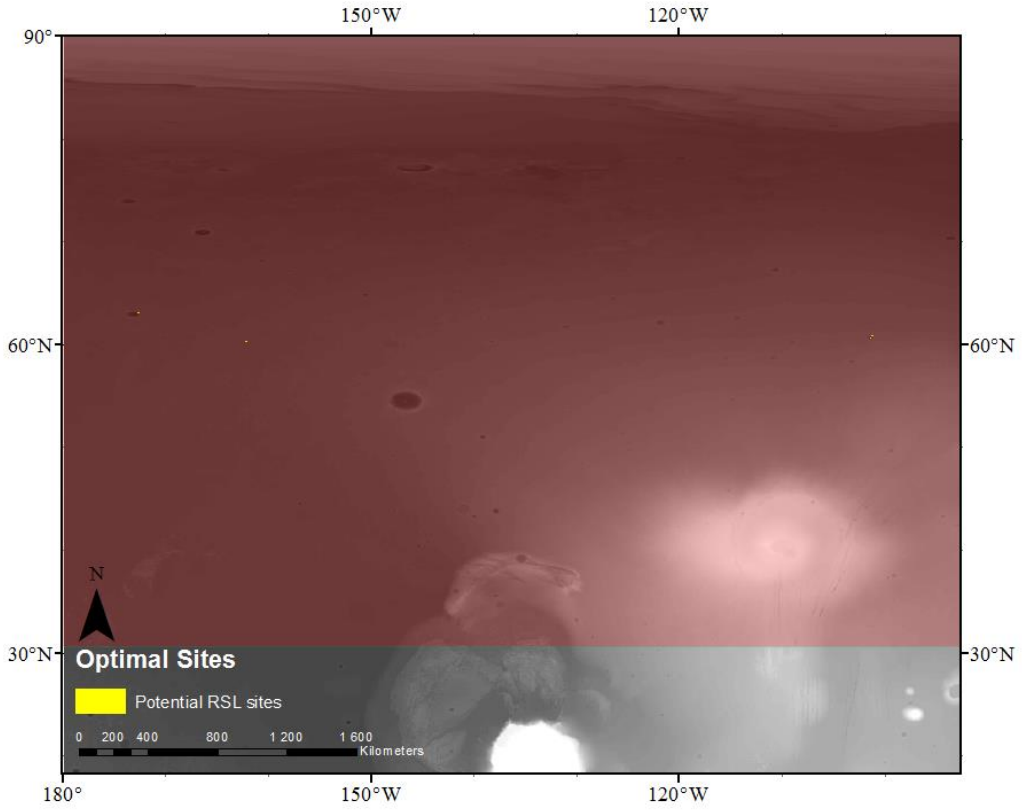

Figure 7: All the yellow areas on the map are the potential RSL sites that were produced by the ArcMap model. The map is located in the westernmost location of the study area (the red color indicate the extent of the study area). Cartographer was Andreas Eriksson. Basemap is a Thermal Emission Spectrometer (TES) image from Christensen et al. (2001) and U.S.G.S. (2014).

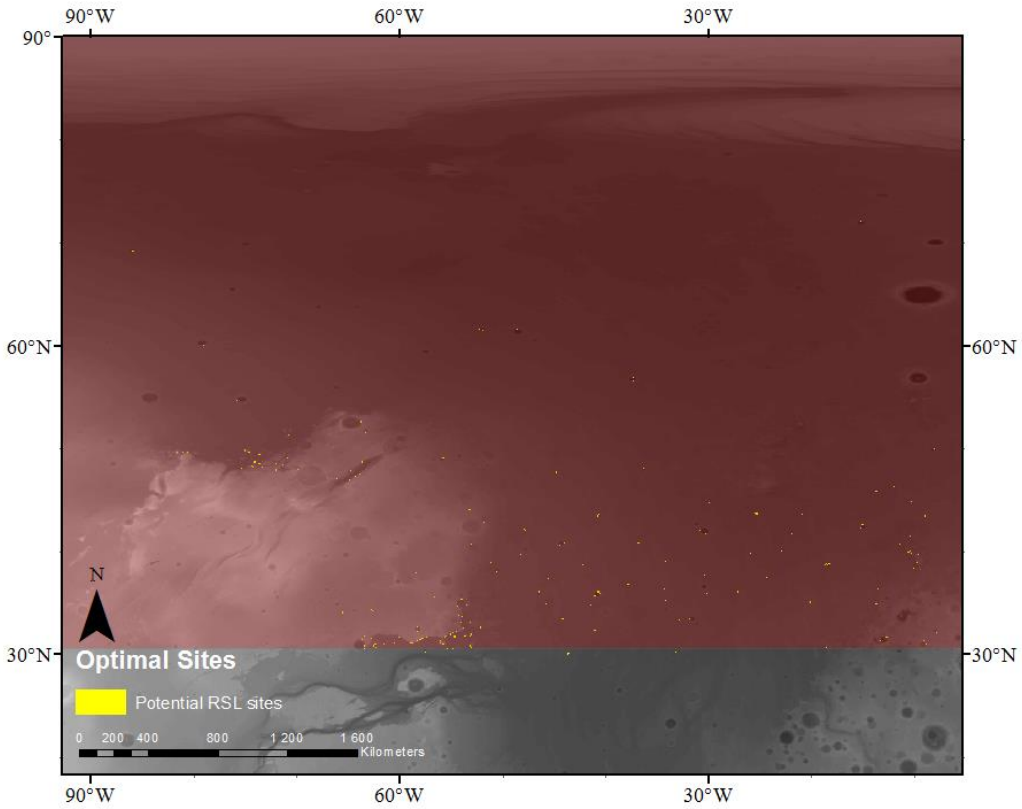

Figure 8: All the yellow areas on the map are the potential RSL sites that were produced by the ArcMap model. The map is located in the western part of Mars but East of figure 7 in the area of Acidalia Planitia (the red color indicate the extent of the study area). Cartographer was Andreas Eriksson. Basemap is a Thermal Emission Spectrometer (TES) image from Christensen et al. (2001) and U.S.G.S. (2014).

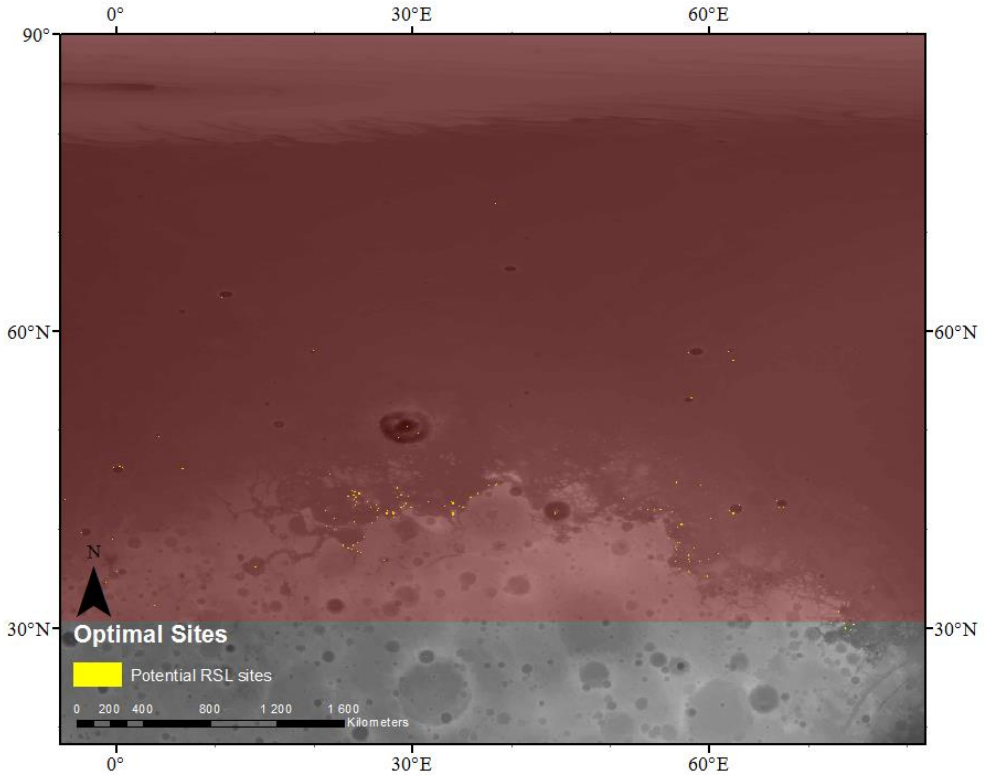

Figure 9: All the yellow areas on the map are the potential RSL sites that were produced by the ArcMap model. The map is located in the eastern part of Mars and East of figure 8. The crater in the middle is the Lyot crater (the red color indicate the extent of the study area). Cartographer was Andreas Eriksson. Basemap is a Thermal Emission Spectrometer (TES) image from Christensen et al. (2001) and U.S.G.S. (2014).

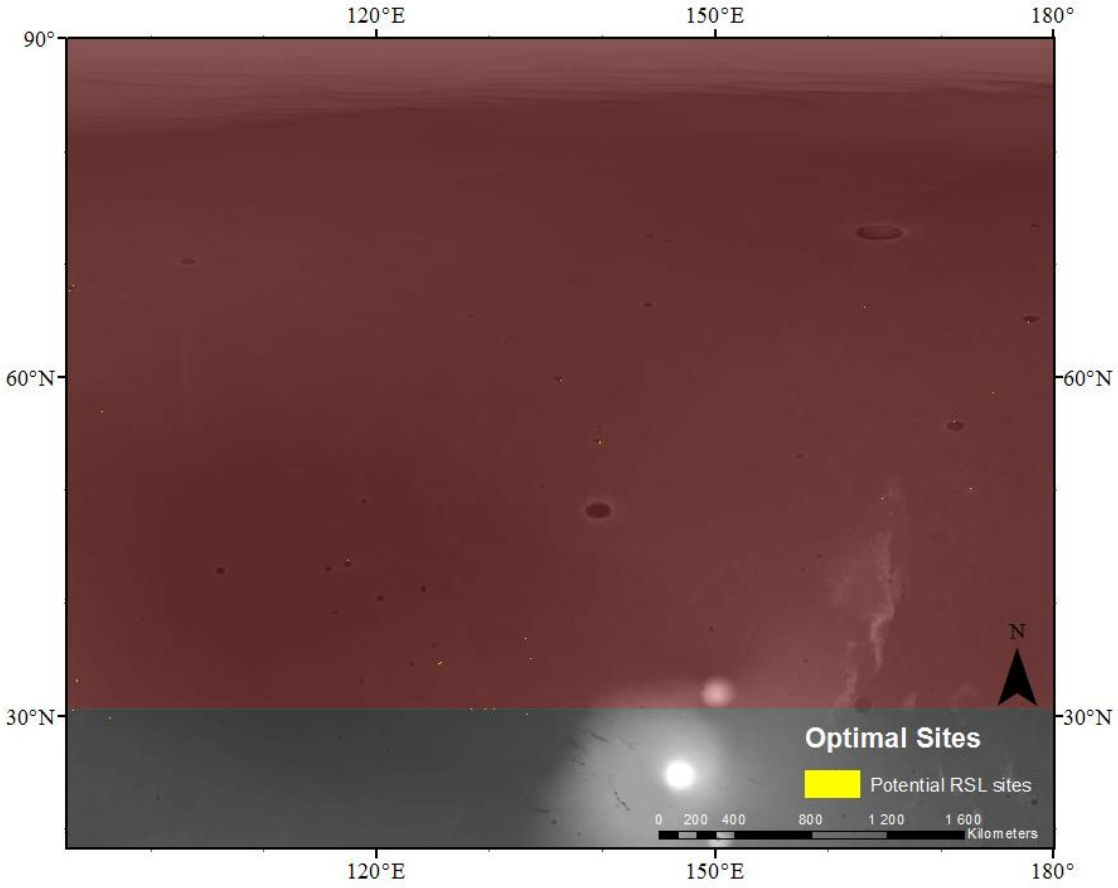

Figure 10: All the yellow areas on the map are the potential RSL sites that were produced by the ArcMap model. The map is located in the easternmost part of Mars and East of figure 9 (the red color indicate the extent of the study area). Cartographer was Andreas Eriksson. Basemap is a Thermal Emission Spectrometer (TES) image from Christensen et al. (2001) and U.S.G.S. (2014).

3.2 Phase 2

With the baseline of 278 optimal sites, images could be acquired from HiRISE. In total 1569 (this number is technically ~785 images since a double set was used for each image as explained in 2.2) images were collected with the help of the ArcMap model. This can be compared to Ojha et al. (2014) who looked at 1984 images from 89°S to 85°N. Examining all the HiRISE images yielded 338 (technically 169) images with potential candidate RSL features. From those images, the extra round of investigations in HiView yielded 94 (technically 47) images that included candidate sites. Important to note is that many of the images are from the same location and were examined multiple times. A total of 27 new candidate sites where established from this (Figure 11).

All candidate sites are confined to the southern part of the northern hemisphere close to the mid-latitudes and the 30°N latitude. Most are found in the areas with the densest population of optimal sites.

No candidate site could be appointed as a confirmed site. However, 5-10 sites could potentially be "partially confirmed" with further investigations. These candidate sites are of higher interest and will be analysed in phase 3 (3.3) of the thesis.

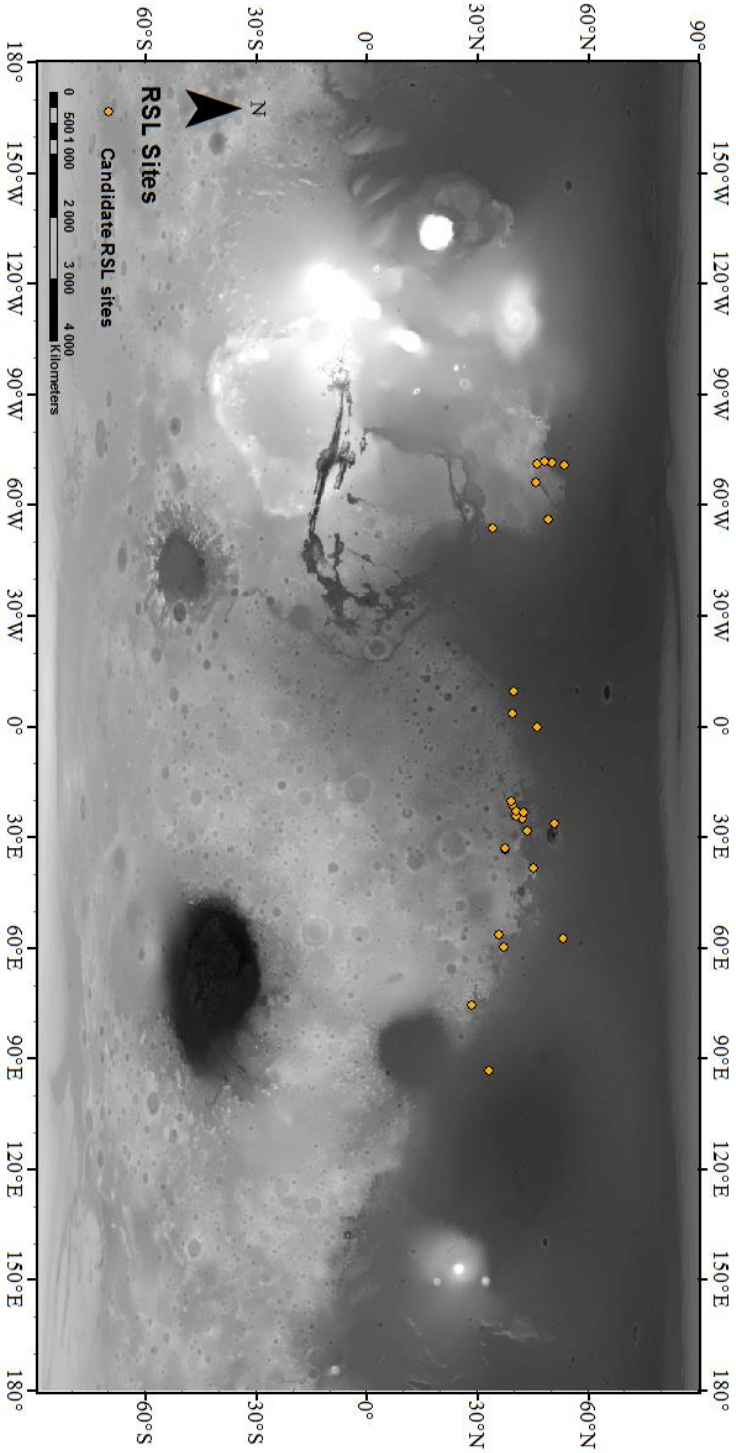

Figure 11: The location of all 27 new candidate RSL sites distributed on the northern hemisphere. Cartographer was Andreas Eriksson. Basemap is a Thermal Emission Spectrometer (TES) image from Christensen et al. (2001) and U.S.G.S. (2014).

3.3 Phase 3

Seven images are used for analysis in phase three. They are as follows; A, B, C, D & E (Table 1). Two images will be used as comparisons namely F which is a confirmed RSL site on the northern hemisphere and G that will be used as a non-RSL standard site (Figure 12) (McEwen et al., 2013).

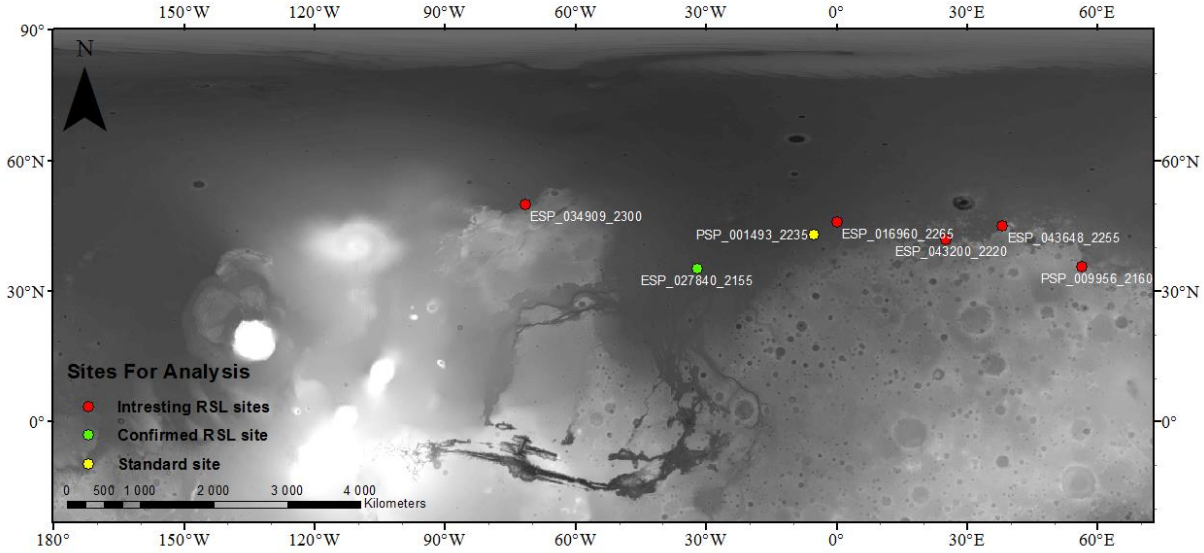

Figure 12: The location of the most interesting sites that this thesis will be testing including the confirmed site in Acidalia Planitia from McEwen et al. (2013) and a standard site location. The labels contain their image name. Cartographer was Andreas Eriksson. Basemap is a Thermal Emission Spectrometer (TES) image from Christensen et al. (2001) and U.S.G.S. (2014).

3.3.1 Temperature data

Most sites are covered by the temperature range 267-278 K which is within the range of RSL parameters. A few of the sites fall within the range of 278-288 K. These include both the confirmed RSL site and the standard site (Figure 13). Temperature readings for all interesting sites can be found in Table 1.

Table 1: Data gathered from the most interesting sites, the confirmed site, the standard site and the Don Juan Pond. Grain size was derived based on the thermal inertia and a graph by Edgett and Christensen (1991). All areas have finer grain sizes. In the temperature measurements most sites are similar as well. The same trend follows in the water vapour data. In the CO_2 data the top four sites in the table have lower values.

ID Code	Interesting Sites	Grain size etc	Thermal inertia	T in Kelvin (Ls=110)	water vapour content (kg/m^2)	CO_2 column (kg/m^2)
A	ESP_034909_2300	Medium sand	308	273,27	0,018	179,87
B	ESP_043200_2220	Fine sand	246	277,58	0,0252	183,21
C	ESP_043648_2255	Silt	134	275,37	0,024	175,87
D	PSP_009956_2160	Fine sand	247	277,14	0,0236	148,45
E	ESP_016960_2265	Silt	84	277,9	0,027	199,43
F	ESP_027840_2155	Fine sand	206	279,86	0,031	197,56
G	PSP_001493_2235	Fine sand	225	279,56	0,027	198,39
DJP	Don Juan Pond	Colluvium	X	223,15-293,15	X	X

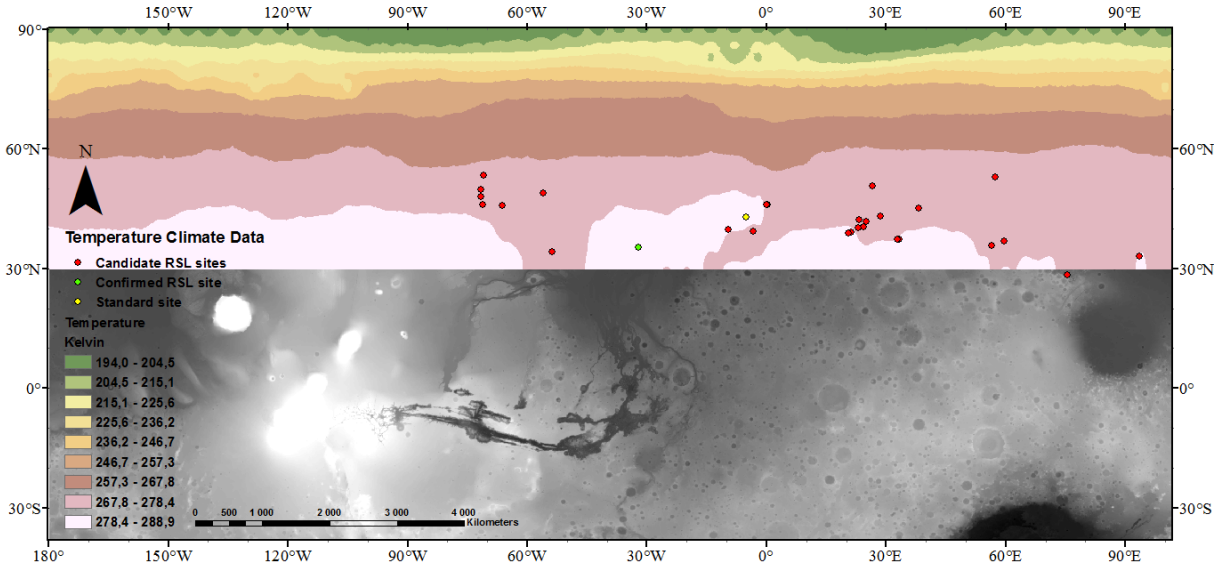

Figure 13: Map of the temperature data distribution on the northern hemisphere. The map includes all sites as well as the confirmed site from McEwen et al. (2013). Most sites are found in the warmer areas on the map closer to the mid-latitudes. Cartographer was Andreas Eriksson. Basemap is a Thermal Emission Spectrometer (TES) image from Christensen et al. (2001) and U.S.G.S. (2014).

3.3.2 Water Vapour and CO_2 column

Atmospheric water in close proximity to interesting sites is lower in the southern region than in the northern region (Figure 14). All the interesting sites in the south are either in the range 0.0159-0.0251 kg/m^2 or the 0.0251-0.0343 kg/m^2. Within these ranges the standard site and the confirmed RSL site can be found. All water vapour readings for each site are available in Table 1.

Data for the CO_2 column is spread out over a wide range of values for all sites. It stretches from around 150 kg/m^2 up to about 200 kg/m^2. All CO_2 readings for each site are available in Table 1.

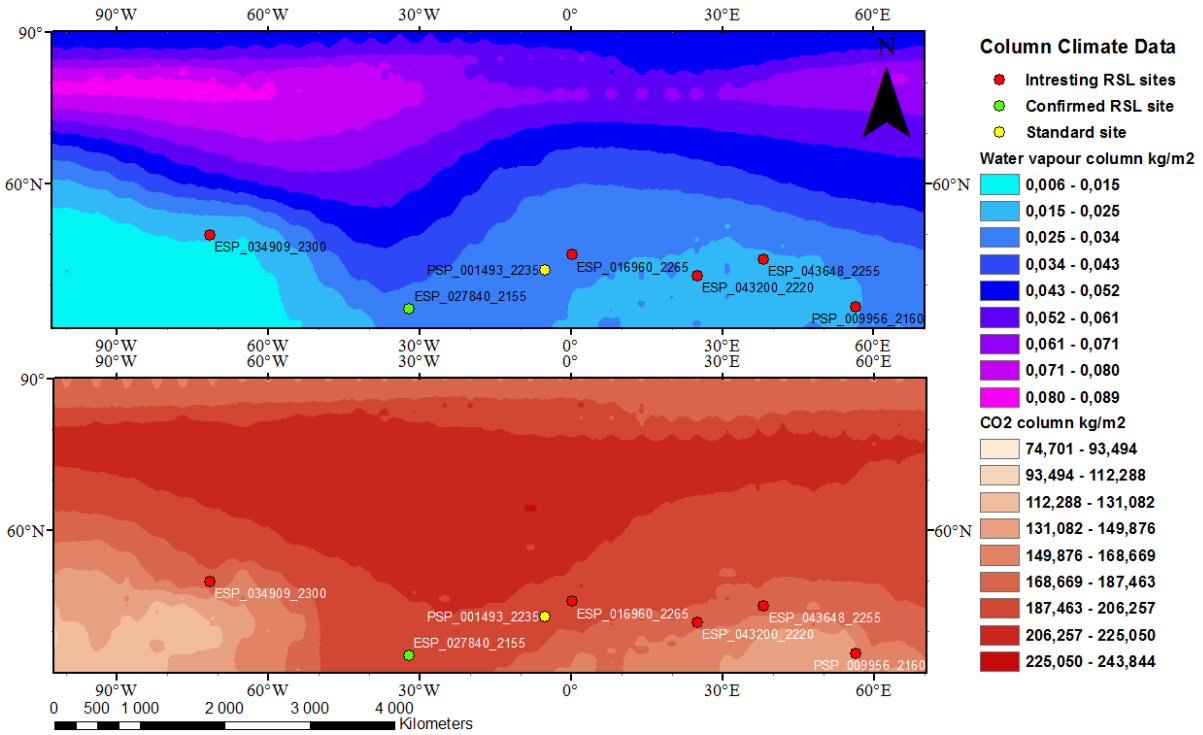

Figure 14: Water vapour data and CO_2 data distribution on the northern hemisphere. This map includes the Interesting sites as well as the confirmed site from McEwen et al. (2013). Most interesting sites are found where there is less water and less CO_2. Cartographer was Andreas Eriksson. Basemap is a Thermal Emission Spectrometer (TES) image from Christensen et al. (2001) and U.S.G.S. (2014).

3.3.3 Overview of studied sites

Most sites include similar surface features and/or landforms. The most prominent feature close to the RSL sites is smaller dunes or ripples. Another feature common for most slopes with candidate RSL are different kinds of flow features (Figure 15). Similar attributes are found in the standard site and confirmed RSL site (Figure 16). Site D only have small features appearing to be alcoves, it is possible that they are newly formed.

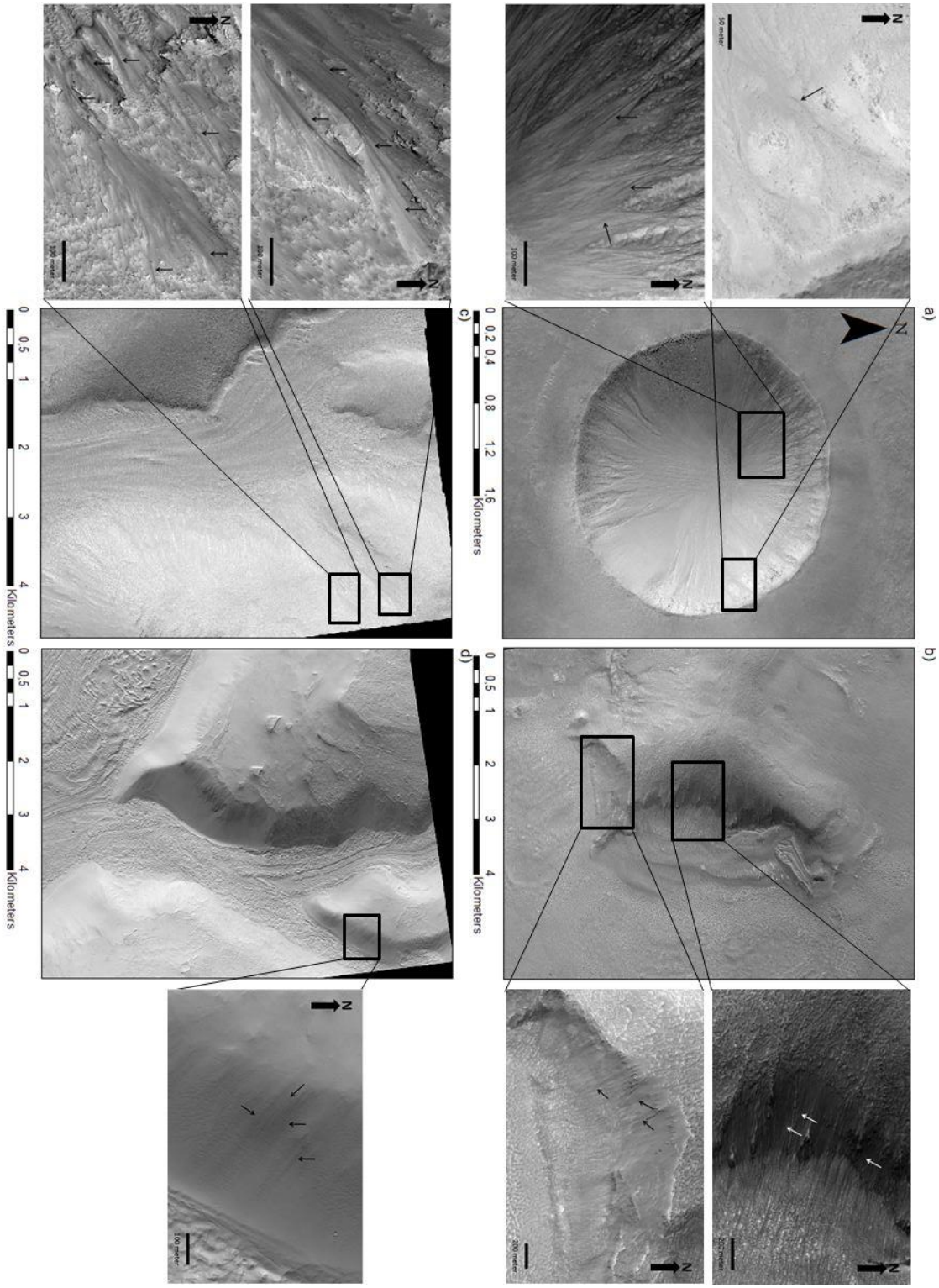

Figure 15: Zoomed in HiRISE images from the interesting sites. Boxes show the location of the inset images. Arrows in inset images point to potential RSL's found in each image. The images are as follows; a) Crater in ESP_034909_2300 (A). Solar incidence angle 43°, with the Sun about 47° above the horizon. b) Slopes in ESP_043200_2220 (B). Solar incidence angle 39°, with the Sun about 51° above the horizon. c) Slopes in ESP_043648_2255 (C). Solar incidence angle 41°, with the Sun about 49° above the horizon. d) Slopes in PSP_009956_2160 (D). Solar incidence angle 45°, with the Sun about 45° above the horizon. Cartographer was Andreas Eriksson. Credit: NASA/JPL/University of Arizona

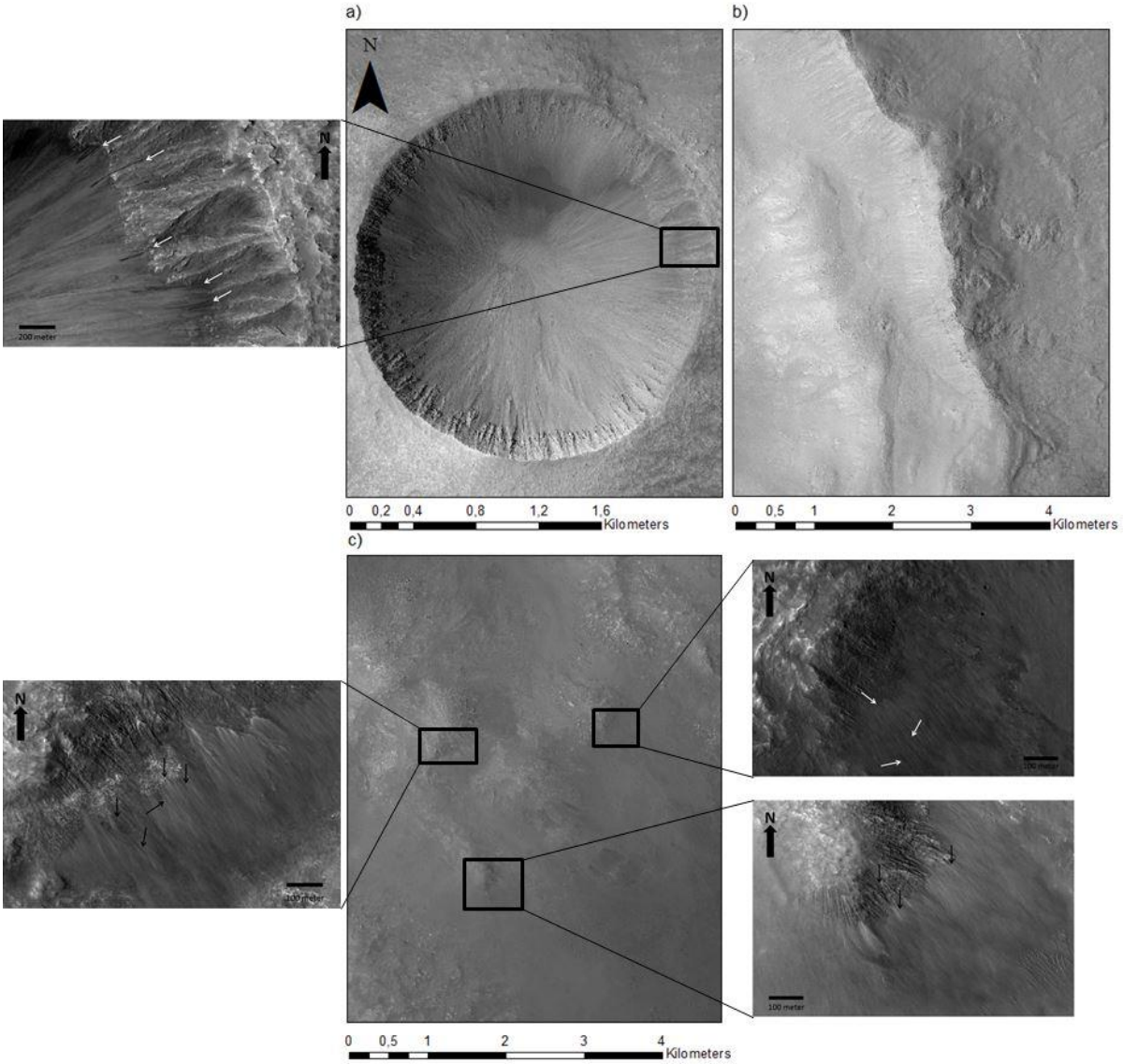

Figure 16: Zoomed in HiRISE images from the interesting sites. Boxes show the location of the inset images. Arrows in inset images point to potential RSL's found in each image. The images are as follows; a) The confirmed site found in ESP_027840_2155 (F) from McEwen et al. (2013) All arrows point at confirmed RSL. Solar incidence angle 48°, with the Sun about 42° above the horizon. b) Area of the standard site from PSP_001493_2235 (G). Solar incidence angle 50°, with the Sun about 40° above the horizon. c) Three different slope areas in ESP_016960_2265 (E) whom all include potential RSL. Solar incidence angle 42°, with the Sun about 48° above the horizon. Cartographer was Andreas Eriksson. Credit: NASA/JPL/University of Arizona

Candidate RSL with similarities to terrestrial 'water tracks' was noted. Most sites only have small to no similarities with the water tracks of DJP. Two sites (A & C) have good similarities with water tracks whilst the confirmed RSL site (F) has high similarities with the water tracks feature. The standard site has no water track similarities at all (Figure 15 & Figure 16).

Compared to the water tracks in DJP, several other surface features occur in close proximity to candidate sites. Colluvium is found in DJP (Dickson et al., 2013) which corresponds to the finer grained material many of the candidate sites is supposed to have.

Similarities to channels can be traced to site D which has potential channels close to the candidate site. Ice within the regolith (Mangold et al., 2016) can potentially be found in several candidate sites and in DJP as an ice-cemented sediment lobe (Dickson et al., 2013). Permafrost is said to be abundant on Mars at most, if not all, latitudes but the depth will most likely differ depending on location (Johnsson et al., 2014). At DJP a permafrost layer starts under about 20 cm of colluvium at a slope to its east (Dickson et al., 2013).

The grain sizes for each sites based on thermal inertia and Edgett and Christensen (1991) provide rather fine grained material (Table 1). For all sites, the grain size is < medium sand.

4. Discussion

4.1 Importance of the ArcMap Model

The ArcMap model in phase 1 is the baseline for this thesis since it is used to find the most suitable areas for RSL occurrences. There are, however, a few problems concerning it. Different settings and small changes could alter many aspects of the model. One example is the basemaps used in the model. A different set could probably change the layout of the optimal sites (Figure 7, Figure 8, Figure 9 & Figure 10). This is also true for other parameters.

4.1.1Reclassing Parameters

The parameters of the model was, as stated in 2.1, set after previous academic works (McEwen et al., 2013; McEwen et al., 2011; Ojha et al., 2014). When the classes were set with the "Reclass" tool, the values of the parameters differed slightly from the set parameters of the model based on academic works (McEwen et al., 2011). One example is the thermal inertia where the classes in the model where set to 133-402 J m^{-2} $s^{-1/2}$ K^{-1} when it was supposed to be 200-340 J m^{-2} $s^{-1/2}$ K^{-1}. However, the important area is still within the set parameters and McEwen et al. (2011) says that the value for thermal inertia is "about" 200-340 J m^{-2} $s^{-1/2}$ K^{-1}. This means the values could probably be more or less in this category.

The other values for slope, albedo and temperature all lay within their set parameters which probably means that changes to the map layout is minimal. Something that could change the map layout or give it a better accuracy as a matter of fact is to add parameters to the model. McEwen et al. (2013) suggest that RSL can occur on equator-facing slopes with bedrock exposures. With these two extra parameters a higher accuracy could be met with the downside of less covered area and the dismissal of RSL that may occur on areas that are not on equator-facing slopes. Using the most prominent parameters for the model seems most

correct and sufficient for this thesis. Other parts of the model might change the layout more drastically like the "Weighted Overlay tool".

4.1.2 Weighted Overlay tool and comparison to the Southern Hemisphere

Results based on the settings from the "Weighted Overlay tool" is compared to confirmed site information from McEwen et al. (2013) and a new model based on the southern hemisphere. As described in 2.1 the setting for slope is set to 60%, for temperature to 20%, for thermal inertia and albedo to 10%. It is necessary that the slope setting is the highest because we need steep slopes in order to have RSLs, however; alterations to the settings may change the areas for the optimal sites. A higher temperature setting would mean that the model recognise that specific parameter more and the map will probably yield bigger areas that is more in comparison to the temperature data. However, after trying to change the settings by altering the percentages no apparent change was found in the map layout created by the model.

Even with the different settings of temperature or slope, the percentages used for this thesis is probably accurate if compared to other confirmed candidate sites. McEwen et al. (2013) have data on several confirmed sites on both the southern and the northern hemisphere. In the north in Acidalia Planitia a confirmed site is in close proximity of several areas the model predicted would be optimal sites. This means the accuracy could be improved but the current accuracy is within an acceptable range. To further develop this statement; in Figure 7, Figure 8, Figure 9 & Figure 10 most of the optimal sites are in craters or on prominent slopes that stands out in the landscape. This means the model has hit slopes, craters and areas that can potentially host RSL. Some of these areas corresponds to McEwen et al. (2013) which means a few areas hosting confirmed RSL was hit or close to being hit by the model. Even if the confirmed site was not hit by the model used by this thesis, this is probably due to the basemap pixel-size of 7409X7409. It is in a favourable crater but this may not be recognised because the crater might be smaller than those sizes and was not accepted in the model to have those parameters. That is mostly the reason why this thesis looks at surrounding areas as well. The model is an estimate of where there might be RSL including areas in close proximity.

In order to see how accurate the model might be, the same parameters were used to find optimal sites in the southern hemisphere (Figure 17). Confirmed sites based on McEwen et al. (2013) were used to see if the optimal sites were in close spatial proximity to them. Through this southern model one can clearly see similar trends when compared to the northern model. The densest areas of optimal sites are in the mid latitudes or in the middle of the map close to

Argyre and Hellas planitia. Most of the candidate sites occur at the optimal sites or within a few kilometres of them (10-30 km), some in the same craters as confirmed sites. This shows the model has an adequate accuracy and can predict areas with interesting features. When doing a quick calculation of how many confirmed sites were in close proximity of optimal sites made by the model, roughly 70% of them were either on an optimal site or a few kilometres away (10-30 km) from one. This does not say too much about the accuracy of the model. However, statistically 70% of RSL's are covered by this model if the statistics are correct. But, as previously noted, not too much information can be derived from this statement and is just used as an example that many RSL sites could be found with the model.

Another important thing to note is that there are a lot more optimal sites on the southern hemisphere. This might be because the area is much larger with the potential of having a lot more available slopes on the heavily cratered southern highlands, however, the number of optimal sites reach a number of 11297 which is 34 times larger than the northern part. This will be discussed more in 4.4. The temperature, however, is a parameter that can change depending on several factors.

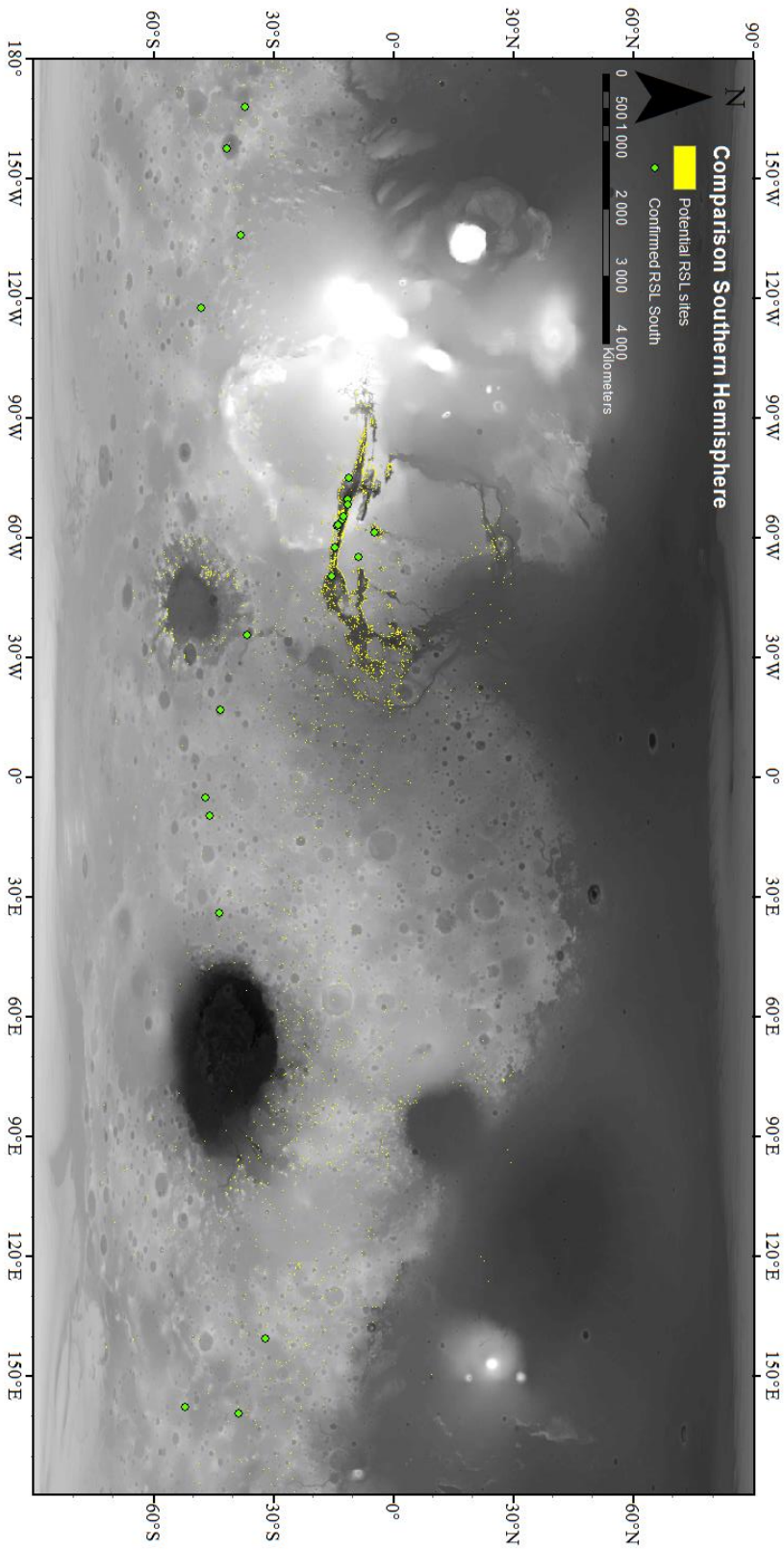

Figure 17: This map features the optimal areas for potential RSL sites on the southern hemisphere and the mid-latitudes. It is based on the ArcMap model used to find areas on the northern hemisphere and is used as a comparison between the two hemispheres. In order to determine any form of accuracy or if the model works, several confirmed sites from McEwen et al. (2013) was added. By determining their proximity to yellow optimal areas an assumption is made on the models accuracy. Cartographer was Andreas Eriksson. Basemap is a Thermal Emission Spectrometer (TES) image from Christensen et al. (2001) and U.S.G.S. (2014).

4.1.3 Differences in the Temperature parameter

Temperature data for the thesis does not correspond to other scientific works about RSL. The same goes for other Martian features and Mars in general. Most papers used data derived from remote sensing satellites orbiting the planet. They are mostly based on images from; the Thermal Emission Imaging System (THEMIS) aboard the 2001 Mars Odyssey spacecraft, the Thermal Emission Spectrometer (TES) aboard the Mars Global Surveyor (MGS) and nadir measurements from the Mars Climate Sounder (MCS) aboard the MRO (Chojnacki et al., 2016; Edwards & Piqueux, 2016; Johnsson et al., 2014; McEwen et al., 2013; Ojha et al., 2014; Stillman et al., 2016; Stillman et al., 2014). This is high quality data under surveillance by high ranking institutions including NASA. Many papers have used this information and pushed knowledge of Mars forward.

If a comparison is made to the MCD one can probably say that instruments such as THEMIS have a higher quality. However, the MCD is a General Circulation Model (GCM) that uses simulations and equations (Forget et al., 1999). A GCM uses equations on the general circulation of the atmosphere in order to make simulations about the climate. Due to all the inputs in the equations and uncertainties regarding changing variations in parameters, a single model can yield different results. The model will however, make a prediction of the climate. They are confirmed by using measured data from other devices and a GCM is good if it is within a specific margin of error (ICPP, 2013).

With the use of a sturdy GCM the MCD can depict good temperature data that can compare with the quality data from other instruments such as THEMIS. In this particular matter the MCD use a GCM that is developed by several departments with close contacts to the European Space Agency (ESA) and the Centre National d'Etudes Spatiales (CNES). The following institutions have helped develop the GCM; Oxford University (UK), Laboratoire de Météorologie Dynamique du CNRS (France), Open University (UK) and Instituto de Astrofisica de Andalucia (Spain) (Forget et al., 1999; Millour et al., 2015). The database is easy to use and Millour et al. (2015) states that the "MCD provides mean values and statistics of the main meteorological variables". This is a perfect fit for this thesis since it is looking at a large area of interest and will not need too much in depth data in this part of the thesis.

When applying the temperature data from the MCD into GIS the IDW interpolation was used. The MCD dataset provided points of temperature data in intervals of ~1.28° along the latitude and 5°-6° along the longitude. Because of this grid of datapoints, IDW was assumed to be the best interpolation to be used on this kind of dataset. The suitability of this method can be discussed since other interpolation methods, one of them being kriging, can provide

more sturdy models (Philip & Watson, 1982; Watson & Philip, 1985). However, when comparing the IDW temperature image (Figure 18) with the Model image made by the MCD (Figure 19), they are strikingly similar.

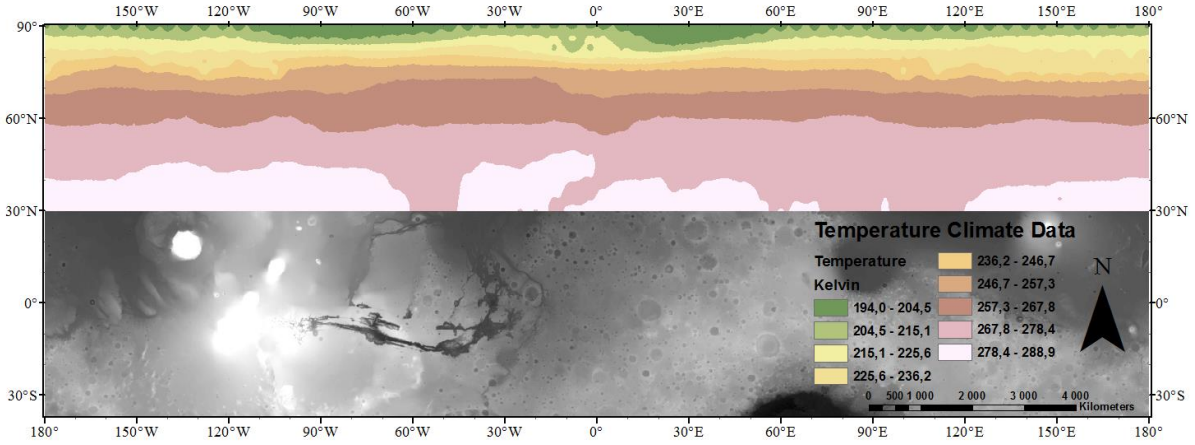

Figure 18: A map of the temperature data on the northern hemisphere for comparison with the MCD data. The comparison is made in order to see if IDW interpolation is good to use for these tests. Both images have strong similarities. Cartographer was Andreas Eriksson. Basemap is a Thermal Emission Spectrometer (TES) image from Christensen et al. (2001) and U.S.G.S. (2014).

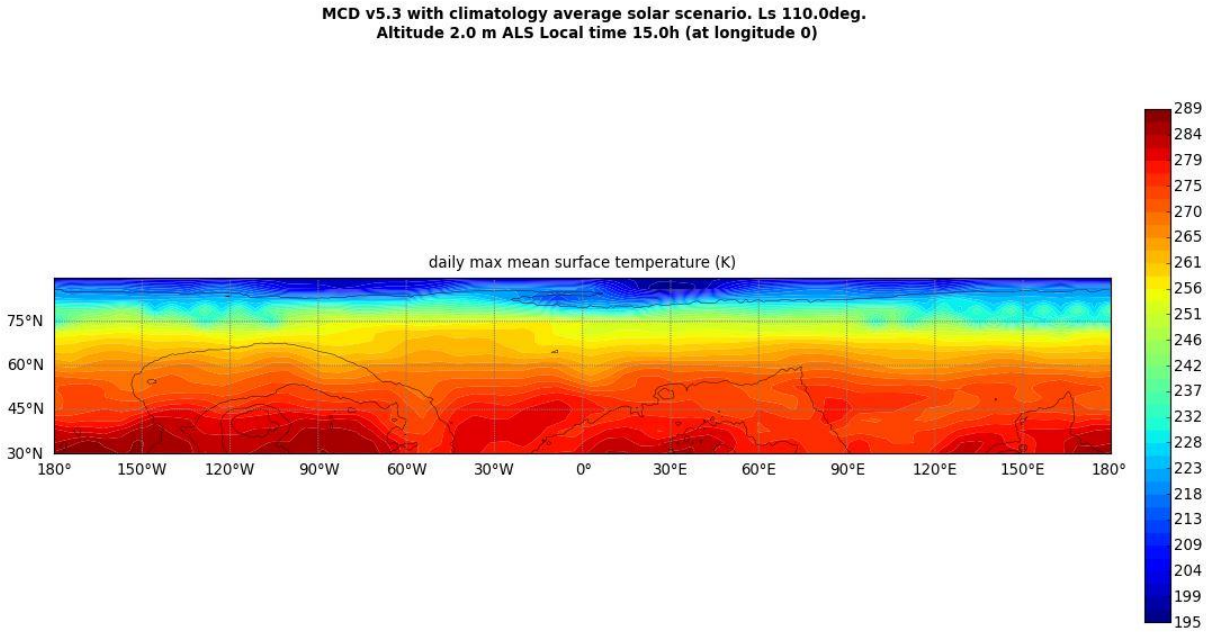

Figure 19: Temperature data from the MCD. It is used for comparison with the northern hemisphere temperature data regarding the use of IDW interpolation on that data. Both images have strong similarities. Image derived from the Mars climate database (MCD).

Similar correlations are true for the IDW image (Figure 20) and the MCD image (Figure 21) in the southern hemisphere. This could indicate that the MCD potentially uses an IDW interpolation approach which means that the IDW interpolation is possible to use in the model that derived the optimal sites for RSL.

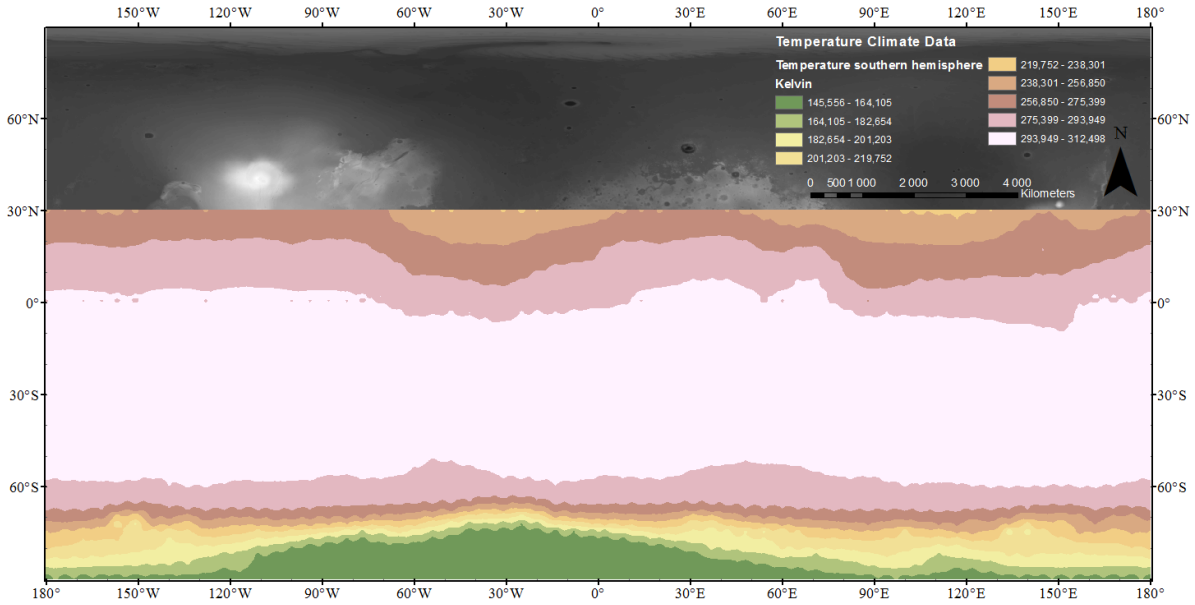

Figure 20: A map of the temperature data on the southern hemisphere for comparison with the MCD data. The comparison is made in order to see if IDW interpolation is good to use for these tests. Both images have strong similarities. Cartographer was Andreas Eriksson. Basemap is a Thermal Emission Spectrometer (TES) image from Christensen et al. (2001) and U.S.G.S. (2014).

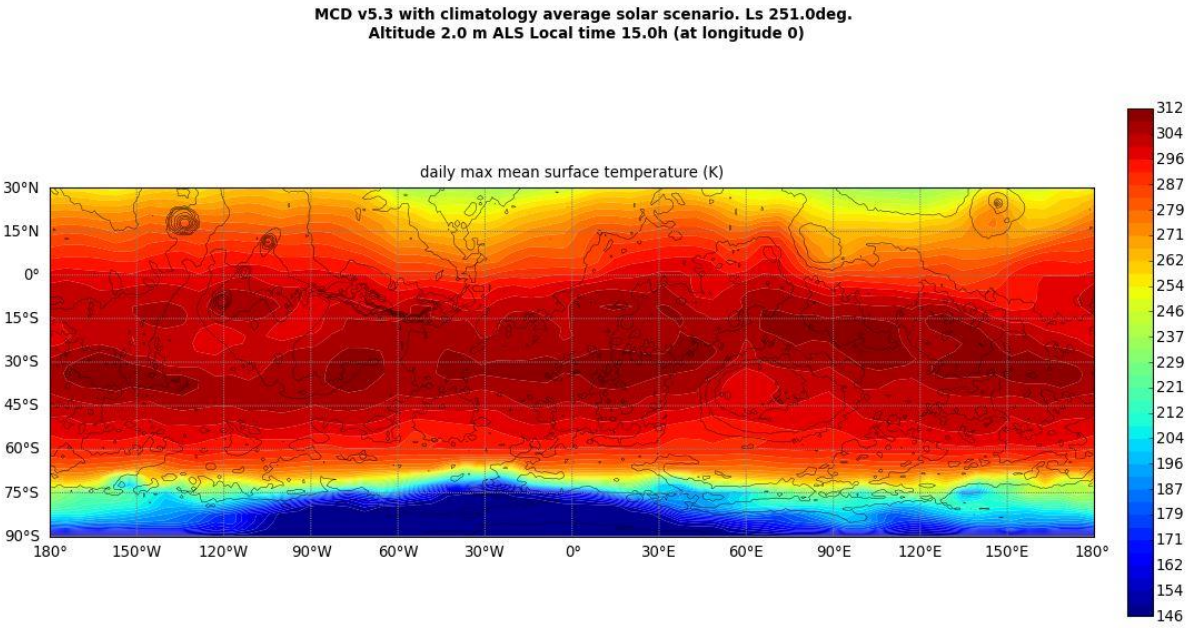

Figure 21: Temperature data from the MCD. It is used for comparison with the southern hemisphere temperature data regarding the use of IDW interpolation on similar data. Both images have strong similarities. Image derived from the Mars climate database (MCD).

An important note to mention about the temperature data is at which time of year it was derived. It was taken around the peak of northern summer at L_s 110 close to the summer solstice at L_s 90. The reason for this is to gain access to the most optimal temperature values at the time when RSL is most active. Changes to L_s could change the temperature values slightly and L_s 90 could potentially have better temperature values. But, it is still during the

same season and RSL should be found either way. The only problem might be that some sites might be lost. This should give good approximate values for the model and that is what this thesis mostly wants as a start.

Naturally, images taken during winter season are important for seasonality studies and will be kept. However, images taken during winter will be easier to exclude as RSL if strong lineae are found within them.

4.2 Problems with new candidate sites

In the process of investigating all the 1569 images, a major challenge when interpreting the RSL is a feature known as slope streaks. They are morphologically similar to RSL and appear as low-albedo slope features. The slope streaks do however not follow seasonal cycles of flow and fading. Slope streaks are typically more distinct in satellite imagery and single flows cover larger slope surfaces. Some other differences are that they can form in any season and are located on slopes with a higher albedo (McEwen et al., 2011). With the model this should not be too much of a problem; however, several areas are located outside of the optimal sites. It is a possibility that a few areas are only slope streaks because of the difficulty of distinguishing them from one another. They cannot be confirmed either since there might be a lack of repeat coverage to determine for example seasonality. This is why it is important to do further studies on the 27 candidate sites in order to better determine their classification.

Another similar problem to the slope streaks is shading. Most of the images are acquired around three a clock in the afternoon (McEwen et al., 2007; Ojha et al., 2014) and many RSL features might be in the shade and be very hard to identify (Ojha et al., 2014). This is especially problematic if there are insufficient images over a certain area.

Sites that are very difficult when considering these problems are gullies. They can host RSL (McEwen et al., 2013; McEwen et al., 2011; Ojha et al., 2014) and in many images dark streak-like features can be observed. It is important to look carefully at those because of shading made by elevation differences next to gully channels. For these reasons all 338 (technically 169) images that were potential candidates were viewed an extra time in the software HiView.

With HiView, minor details could much easier be identified and several slope features that have uncertainties can be discarded as they do not meet the criteria for RSL. It takes advantage of JPEG2000 images that can be rendered in such a way that only the area that is displayed or zoomed in to is rendered. While it does this the other parts of the image is left unloaded (Castalia, 2012). The computer can thus processes high resolution images without

problem. One example is Figure 22 where one can clearly see boulders and debris without much effort. This is how uncertain areas from the potential candidates were discarded as a closer inspection found they were not true dark streaks and thus were not RSL.

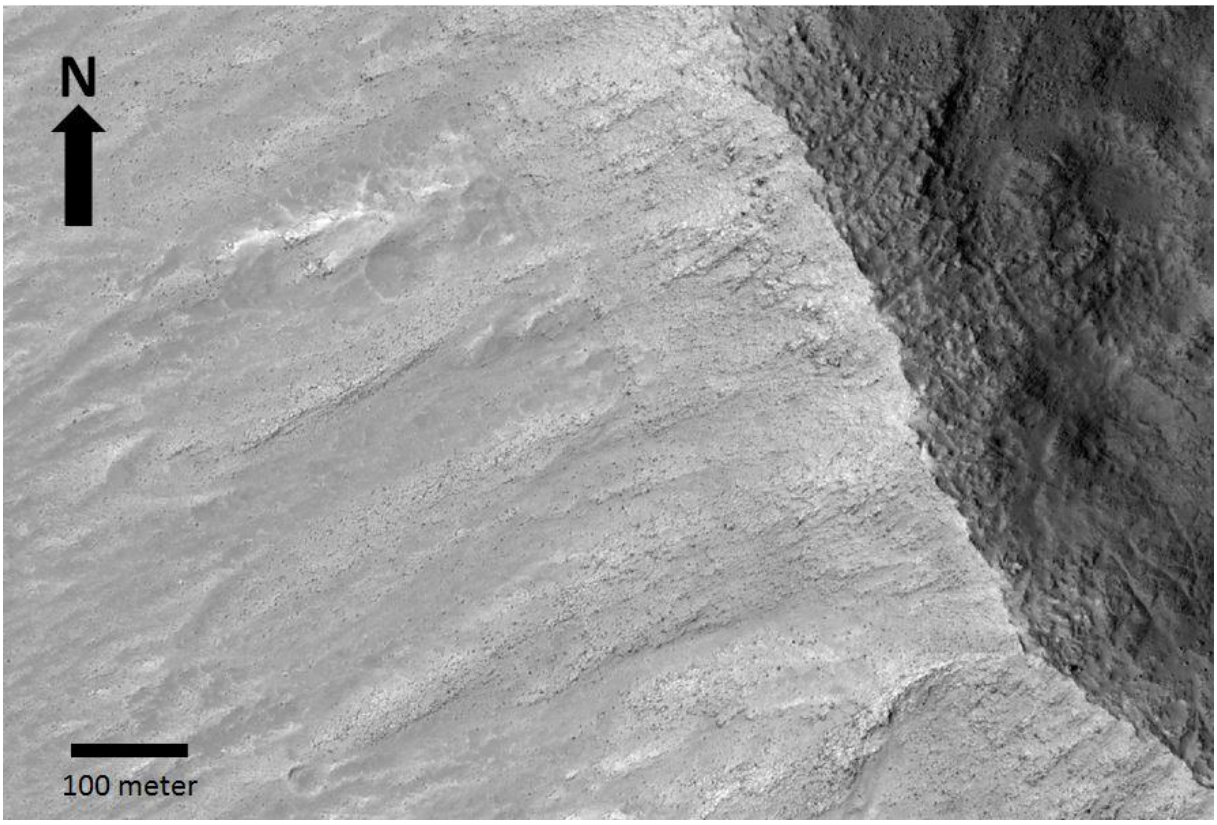

Figure 22: Hiview image of PSP_001493_2235 (I). It is possible to clearly see separate boulders and debris going down the slope. This is possible in general on images without slopes as well. The slope downward direction is SW. Solar incidence angle 50°, with the Sun about 40° above the horizon. Credit: NASA/JPL/University of Arizona.

4.2.1 Lack of HiRISE images

As mentioned previous in 4.2, there are problems with insufficient data. This is because there can be a lack of coverage over a certain area. The HiRISE instrument has imaged areas for about 12 years. Despite its high resolution and impressive database, there are areas that are not covered or only have one image in that local area. This is problematic in the classification of RSL.

Without images over a Mars year where a minimum of five would suffice (McEwen et al., 2011), it will be difficult to see seasonal changes such as incremental growth or recurrence. For this thesis, many of the candidate sites only have one image. One example is image A. Despite being an interesting candidate it cannot be classified as partially confirmed unless complementary images can prove this. It is however, possible to get more images over a certain area.

The HiRISE website, maintained by the University of Arizona, contains the option HiWish. With this it is possible for anyone to suggest potential areas the HiRISE instrument

should focus on. The problem is that it can take a while based on prioritised images, flight plan of the satellite and long queue times because of many suggestions.

For this study the coverage at certain locations was not satisfactory. This is mainly because a majority of images are focused around areas of interest such as Valles Marineris or the Gale crater. This is good for many other scientific studies that focus on smaller areas. For RSL research in Valles Marineris there is good cover and a lot of data can be accumulated. In these cases, classifications can be done with no trouble. This is very notable in studies by McEwen et al. (2011), McEwen et al. (2013), Stillman et al. (2016) and Ojha et al. (2014). These studies have big dataset to start from and hundreds of images over an area where 20-40 images are over the same location. The academic works can make good interpretations from this and thus classify confirmed sites. This is one of the main differences between this thesis and other studies. There is insufficient coverage over the same area in many of the optimal sites. Image A and another image known as ESP_033854_2335 only have one image covering them whilst image ESP_044677_2310 for example have at least 8 images covering that area. Despite this, 27 new candidate sites for further study were established.

4.2.2 Comparing Candidate sites

In other studies such as Stillman et al. (2016) a wide range of RSL sites can be found. Many of these are located in the mid-latitudes close to the equator which corresponds to the optimal sites found in the models (see 4.1.2 and Figure 7, Figure 8, Figure 9 & Figure 10). They are also found in Chryse Planitia, Acidalia Planitia and in the southern mid-latitudes and range from many different classifications of RSL. If the latitudinal setting of the RSL from Stillman et al. (2016) is compared with the RSL found in this thesis, a match of similar latitudinal locations can be found. The only problem is that no RSL sites are registered outside of Chryse –and Acidalia Planitia in the report by Stillman et al. (2016), which mean that they probably did not look at other regions. This is the area where most of the candidate sites are located in this thesis and can be hard to use as a comparison. This might, however, be turned around and used as a strength of the thesis.

It is hard to make correlations of sites in the northern hemisphere since most reports mainly focus on the south. In Ojha et al. (2014) there are many observations over both hemispheres. However, this study only investigated images in Mars year 30 between L_s 250-360° and in Mars year 31 between L_s 0-10°. These images were mostly taken from the areas located in the southern hemisphere. This means many observations where discarded that could

potentially have RSL in the north since northern summer mostly occur around L_s 110° (Mangold et al., 2016).

The same pattern can be found in Stillman et al. (2014), McEwen et al. (2011) and McEwen et al. (2013). Image data is only covering southern areas or the equator and are not close to the candidate sites found in this thesis. The only northern sites are those in Acidalia- and Chryse Planitia. This makes comparisons and correlations difficult and cannot provide support to sites found in this thesis.

4.3 Are the candidate sites wet flows or dry flows?

Processes that create RSL are highly debated. The reason that RSL's have gained so much research attention is the possibility that liquid water is the formative agent (McEwen et al., 2011). This notion is countered by hypotheses that proposes dry granular flows with only limited role of water in the formation of RSL (Dundas et al., 2017). A hypothesis is going to be made about a few of the discovered candidate sites based on these statements. The hypothesis aims to determine the most likely formative process of RSL at the studied sites.

4.3.1 Salt deposits

A problem with determining whether the candidate sites are wet flows or not is the lack of salt data. On the Martian surface, perchlorate salts are present at a global scale. It was discovered by the Phoenix lander and opened up new possibilities for liquid water on Mars (Gough, Chevrier, Baustian, Wise, & Tolbert, 2011; Mangold et al., 2016). Perchlorate salts, and salt deposits, in general are important for the creation of brines and deliquescence. On Mars today it is mostly found in the regolith and is supposed to be widely distributed on the Martian surface. An example is that it was detected in the Gale crater (Martín-Torres et al., 2015).

The studied sites in this thesis do not have any perchlorate data available. However, if it is assumed that perchlorate salts are to some degree homogenously distributed over Mars surface, it will be easier to determine possible brine formations that may show if we have wet flows or not. According to Martínez and Renno (2013) three things are needed to form brines; To be able to have deliquescence and creation of brines, salts are needed at the location, a temperature over the eutectic temperature (T_e) for the specific salt, and the relative humidity (RH) has to exceed the deliquescence relative humidity (DRH). T_e is the point the temperature can reach at its lowest where the aqueous solutions are still stable (Gough et al., 2011).

4.3.2 Possibility of Deliquescence

In order for deliquescence to occur RH must be higher than DRH for the perchlorate salt (Gough et al., 2011; Martínez & Renno, 2013). Laboratory testing of the perchlorate salts

$NaClO_4$ and $Mg(ClO_4)_2$ by Gough et al. (2011) provided DRH values depending on different temperature values. The low water vapour values would normally not create brines through deliquescence; however, the Martian atmosphere can become oversaturated. The atmosphere is cold and thin and can saturate easy since only a small amount of water vapour is necessary (Forget, 2007; Mangold et al., 2016). This means that only small amounts of water vapour are needed to obtain higher RH values than DRH.

For the interesting sites A-E, this means that the low water vapour values have a possibility of deliquescence. This is further developed by Raack et al. (2017) who claims that it is possible to have lower amounts of liquid water since the values needed are supposedly overestimated. This means that potentially all tested sites could develop brines and thus might be water based RSL.

When compared to the confirmed site in Acidalia Planitia, all tested sites have slightly lower water vapour values. They are still in close range of each other which could mean that they are water based. This is taken further by Stillman et al. (2016) who suggest a briny aquifer as a source for RSL. This means that the possibility for brines in the tested sites is good.

Another thing that is in favour of brines and RSL in general in the tested sites is that most of the temperature values are slightly above 273.15 K (or 0°C). The temperature values works well with earlier studies which set the parameters for RSL to be around 250-300 K (McEwen et al., 2011). Because of the high temperatures, ice in the regolith (Mangold et al., 2016) could potentially melt and be a source of water for wet flows of RSL.

The brines themselves benefit from higher temperatures. According to Möhlmann and Thomsen (2011) temporary brines or cryobrines (frozen brines) are possible at low temperatures. This suggests that melting of cryobrines could give wet flows in the tested sites. He further states that cryobrines liquid phase can form through deliquescence which fits in with the potential deliquescence in the tested sites of this thesis (D. T. F. Möhlmann, 2011).

At to low temperatures liquid fluids will not be stable and it will be hard to form brines. This happen if the temperature is close to the lowest T_e values for salts, where a few can reach below 210K (Martínez & Renno, 2013). The right salts (for example magnesium perchlorate ($Mg(ClO_4)_2$) with a T_e of 206 K or calcium chloride ($CaCl_2$) with a T_e of 223.2 K (Chevrier & Rivera-Valentin, 2012)) need to be available for the possibility of brines to form from deliquescence which mean a dry flow might be more likely if this is the case in such areas.

Edwards and Piqueux (2016) argues that temperature measurements taken from THEMIS points toward a dry flow mechanism. Due to high changes in temperature, brines

will freeze and the water will evaporate or sublime. They basically rule out sufficient amounts of water at near surface areas in correlation with RSL. This thesis used “average max mean daily temperature data” at the most suitable time for RSL to be visible during northern summer (L_s 110). Since an average was used it is difficult to determine temperature changes in certain areas and thus problematic to make suggestions based on it.

4.3.3 Grain size

A hypothetical grain size for each tested site was made based on a diagram (Figure 6) by Edgett and Christensen (1991). When tested, it is important to note that surfaces that look smooth in aerial imagery may in fact be rocky. This makes the grain size assumption purely hypothetical.

The sites range between medium sand and silt. Compared to the tested site in Acidalia Planitia they are similar. The confirmed site is supposedly fine sand which corresponds with sites B and D. Overall they are all similar. The fine grain sizes could hold water due to pore space, pore pressure and similar processes and that suggest water based RSL formative processes, but finer grain sizes also point towards dry flows as described below.

According to Dundas et al. (2017) RSL features are close to the angle were cohesionless-sand stops. He is further arguing about similarities in angle of repose and processes on dunes. As previously stated the tested sites have fine grain sizes and they correspond to Dundas et al. (2017). It is also true that changes in grain size can darken the area (McEwen et al., 2011). This suggests that RSL could be dry flows since any creation of water at only the top of dunes seems unlikely (Dundas et al., 2017).

There is a possibility for a mix of the two types of flow. Raack et al. (2017) suggest a levitation method of wet sediment that can lead to grain avalanches. The levitation effect is supposedly activated through boiling of transient water. This works well with the results of the tested sites since they point to both dry flows and wet flows. Another aspect it works well for is the water vapour since; Dundas et al. (2017) states that water has a limited role and Raack et al. (2017) claims that less water is needed due to increased sediment transport because of the levitation process. This means that the low values of water vapour may still be valid for RSL.

The claim that less water is needed works well for potential water ice found in the regolith. Only small amounts need to be available to the different processes described above.

4.3.4 Don Juan Pond Analogy

As mentioned in 1.2 the analogy for RSL is the 'water tracks' found at DJP (Dickson et al., 2013; Levy, 2012). Most of the tested sites only have small similarities to the water tracks in the DJP. After the images of the tested candidate RSL's were compared to the water tracks in DJP, it was hard to identify them as water tracks. The only site that somehow relate to the water tracks of DJP is the confirmed site in Acidalia Planitia. Still, the shape in comparison (Figure 16a) is hard to justify as water tracks despite all the similarities. The shape of the lineae is more erratic in DJP and do not follow similar flow patterns which suggest that they do not fully compare with each other. If however, the candidate site can show more resemblance, water tracks are a plausible comparison. The only problem would be that high soil moisture and water is necessary in the regolith. This would be possible with ice (Mangold et al., 2016) and some studies promote the flow of liquid through the regolith (Levy, 2012), whilst other studies claim water in the near surface is not at elevated levels (Edwards & Piqueux, 2016).

Another part to the DJP discussed by Dickson et al. (2013) is the possibility of snow trapped in alcoves. Potentially these alcoves may house ice that can remain and melt at another time. This is one of the ways that the water tracks may get a water supply from among other processes. This hypothesis could explain seasonality and water supply in RSL. If, however, this could happen, several of the tested sites have potential alcoves as well as the confirmed site. One site (D) is uncertain and may only have small alcoves which suggest that this process is uncertain to be active in this region. Alcoves are potential in the confirmed site as well, but since there are more differences here such as the comparison of the water tracks explained above, no clear feature can be determined from the alcoves.

The DJP colluvium fits very well into the tested sites as well as the confirmed site. This could point towards the wet flow idea; however, it goes well with Dundas et al. (2017) as previously stated in 4.3.3. This means that both types of flow are possible.

DJP is a very saline water source. Dickson et al. (2013) promotes a briny flow through the soil above the permafrost as a source of water and salinity to DJP. One of these flows is the water tracks. The potential for briny flows within the tested sites are favourable. Dickson et al. (2013) further suggest that the hydrological system of the DJP is achievable on Mars near RSL locations if the conditions for it exist. In most locations this is plausible. One example of a parameter is the temperature values which fit well with most sites. Another thing it somewhat counteract is the problems of temperature differences that Edwards and Piqueux

(2016) points out. But it is important to note here that processes on Mars may be different from those on Earth.

The standard site has many similarities to both the tested sites and the confirmed site. The only thing it lacks is any form of lineae or water tracks. This means that areas may still have similar parameters and still not host RSL. This may be due to several factors such as lack of perchlorate salts or liquids in the regolith. However, the candidate sites are potentially RSL due to the lineae and the similarities with other confirmed sites.

Overall a wet process is suggested for the tested sites when compared to DJP. But, since most candidate RSL sites, according to the results made by this study, do not resemble water tracks to that extent it is hard to make that assumption. The best solution would be to say that a combination of both types of flows as described by Raack et al. (2017) above is responsible for RSL based on the information provided in this thesis.

4.4 The Northern Hemisphere in comparison to the Southern Hemisphere

As many studies focus on RSL in the southern hemisphere (Chojnacki et al., 2016; McEwen et al., 2013; McEwen et al., 2011; Ojha et al., 2014; Stillman et al., 2014), fewer works are conducted in the northern hemisphere (Stillman et al., 2016). It seems to be less RSL in the north than in the south. Mangold et al. (2016) and Carr and Head (2010) mention a reason known as the dichotomy (see 1.3) that can be linked to the scarcity of RSL in the north. The difference in elevation between north and south is a crucial component. After investigating areas in the northern hemisphere, the southern hemisphere has more abundant high-relief topography such as valleys, hills and craters than in the north. This provides more ample areas for RSL to form whereas the surface in the northern hemisphere is generally smoother with fewer craters, except for the dichotomy relief at lower latitudes. Carr and Head (2010) points out that crater density is similar on both hemispheres since old craters may be buried beneath the surface in the northern hemisphere. Exhumed craters are highly weathered and eroded as many other older craters. This probably means that weathering and angle parameters may not be sufficient in those craters to form RSL. This dichotomy may be a reason why many more RSL are created in the south.

In 4.1.2 the comparison of optimal sites between north and south was discussed. The amount of optimal sites was many times larger in the south than the optimal sites found in the north (Figure 7, Figure 8, Figure 9 & Figure 10). Some of the sites included were of the mid-latitudes. If the mid-latitudes are disregarded there are still ~25 times as many optimal sites in

the south. This coincide with the earlier statement about the dichotomy that the highlands have more potential to form RSL.

The amount of optimal sites on each hemisphere connects to the amount of HiRISE images currently available. When tested both north and south have similar amounts of images. The problem is that the clusters of images are over currently interesting areas and many areas only have one image. This suggests that repeated image coverage over one location could help improve the amount of RSL found in the north.

Temperature measurements reveal that there are larger areas where RSL can be stable in the south (Figure 20) than in the north (Figure 18). This could be an additional reason for the lack of RSL in the north. The mid-latitudes are promising on both hemispheres which are noted in this thesis as well as in McEwen et al. (2011), Chojnacki et al. (2016) and Stillman et al. (2016). It is further acknowledged by McEwen et al. (2013) that most confirmed sites are in the mid-latitudes and on the southern hemisphere which means that the possibility for RSL is greater in the south. Even so more sites are possible in the northern mid-latitudes (Stillman et al., 2016) and as the search continues, more RSL will probably be found in those areas.

5. Conclusion

Most studies on RSL to this day were focused on the southern hemisphere or the mid-latitudes (Chojnacki et al., 2016; McEwen et al., 2013; McEwen et al., 2011; Ojha et al., 2014; Stillman et al., 2016; Stillman et al., 2014). A few of them touched the northern hemisphere but did not make more thorough investigations. Through the use of a GIS ArcMap model and the HiRISE instrument, 27 new potential RSL candidate sites were found on the northern hemisphere.

There is currently a heated debate regarding the formative process of RSL as either wet or dry flows. Previously, most studies have argued towards wet flows although many aspects of a water hypothesis still remain unresolved. For this reason several of the newfound sites were investigated whether wet or dry flows are more likely. By investigating some of the more interesting candidate sites in this study, it is evident that both models work to some extent to explain the RSL. Based on the model made by this study, physical context and image analyses in this thesis, a combination of wet and dry mechanisms is proposed. The results in this thesis may be in agreement with Raack et al. (2017) which propose a mechanism by levitation of saturated sediments due to vapour from boiling effects.

Through this thesis it is shown that the scarcity of RSL on the northern hemisphere is mostly based on the lack of areas for RSL to form (i.e. fewer available slopes). A main reason might be the dichotomy which shows that optimal sites for RSL are more abundant in the southern hemisphere than in the Northern hemisphere as shown in Figure 17. Less coverage by HiRISE of topographic features in the north compared to the southern hemisphere and fewer areas with the favourable temperatures for RSL may also be important factors that there is currently less confirmed RSL in the north.

More HiRISE images with repeat coverage will be needed to confirm whether the model presented in this thesis made accurate predictions. With more images an accurate assumption can be made to the classification of the RSL sites. Especially for the sites that only had one HiRISE image covering them. With a widened area of coverage it may be possible to find more RSL sites on the northern hemisphere.

Finally, a further investigation into the combined model for the creation of RSL is necessary in order to help solve the uncertainty behind RSL. This will help in providing new information and observations about Mars.

6. Acknowledgments

First and foremost I would like to thank my supervisor Andreas Johnsson for the opportunity to work with this master thesis and for his counselling throughout the project. I would also like to thank Alexander Walter for help with the GIS software ArcMap. Special thanks to John Eliasson and Gustav Tennby for interesting inputs and advice during the project. Finally, I would like to reach out to the University of Arizona and the crew managing the HiRISE instrument as well as the crew managing the Mars orbital data explorer. Without them, NASA and ESA, this project would not be possible.

7. References

Carr, M. H., & Head, J. W. (2010). Geologic history of Mars. *Earth and Planetary Science Letters, 294*(3), 185-203. doi:https://doi.org/10.1016/j.epsl.2009.06.042

Carr, M. H., & Head, J. W. (2015). Martian surface/near-surface water inventory: Sources, sinks, and changes with time. *Geophysical Research Letters, 42*(3), 726-732. doi:10.1002/2014GL062464

Castalia, B. (2012, January 26, 2012). HiView User's Guide Introduction. Retrieved from http://pirlwww.lpl.arizona.edu/software/HiView/Users_Guide/Introduction/Introduction.html

Chevrier, V. F., & Rivera-Valentin, E. G. (2012). Formation of recurring slope lineae by liquid brines on present-day Mars. *Geophysical Research Letters, 39*(21), n/a-n/a. doi:10.1029/2012GL054119

Chojnacki, M., McEwen, A., Dundas, C., Ojha, L., Urso, A., & Sutton, S. (2016). Geologic context of recurring slope lineae in Melas and Coprates Chasmata, Mars. *Journal of Geophysical Research: Planets, 121*(7), 1204-1231. doi:10.1002/2015JE004991

Christensen, P. R., BandField, J. L., Hamilton, V. E., Ruff, S. W., Kieffer, H. H., Titus, T. N., . . . Greenfield, M. (2001). Mars Global Surveyor Thermal Emission Spectrometer experiment: Investigation description and surface science results. *Journal of Geophysical Research: Planets, 106*(E10), 23823-23871. doi:10.1029/2000JE001370

Costard, F., Séjourné, A., Kelfoun, K., Clifford, S., Lavigne, F., Di Pietro, I., & Bouley, S. (2017). Modeling tsunami propagation and the emplacement of thumbprint terrain in an early Mars ocean. *Journal of Geophysical Research: Planets, 122*(3), 633-649. doi:10.1002/2016JE005230

Dickson, J. L., Head, J. W., Levy, J. S., & Marchant, D. R. (2013). Don Juan Pond, Antarctica: Near-surface CaCl2-brine feeding Earth's most saline lake and implications for Mars. *Scientific Reports, 3*, 1166. doi:10.1038/srep01166

https://www.nature.com/articles/srep01166#supplementary-information

Dundas, C. M., McEwen, A. S., Chojnacki, M., Milazzo, M. P., Byrne, S., McElwaine, J. N., & Urso, A. (2017). Granular flows at recurring slope lineae on Mars indicate a limited role for liquid water. *Nature Geoscience, 10*(12), 903-907. doi:10.1038/s41561-017-0012-5

Edgett, K. S., & Christensen, P. R. (1991). The particle size of Martian aeolian dunes. *Journal of Geophysical Research: Planets, 96*(E5), 22765-22776. doi:10.1029/91JE02412

Edwards, C. S., & Piqueux, S. (2016). The water content of recurring slope lineae on Mars. *Geophysical Research Letters, 43*(17), 8912-8919. doi:10.1002/2016GL070179

Forget, F. (2007). Water and Climates on Mars. *Lectures in Astrobiology, 2*, 103-122. doi:10.1007/10913314

Forget, F., Hourdin, F., Fournier, R., Hourdin, C., Talagrand, O., Collins, M., . . . Huot, J.-P. (1999). Improved general circulation models of the Martian atmosphere from the surface to above 80 km. *Journal of Geophysical Research: Planets, 104*(E10), 24155-24175. doi:10.1029/1999JE001025

Gough, R. V., Chevrier, V. F., Baustian, K. J., Wise, M. E., & Tolbert, M. A. (2011). Laboratory studies of perchlorate phase transitions: Support for metastable aqueous perchlorate solutions on Mars. *Earth and Planetary Science Letters, 312*(3), 371-377. doi:https://doi.org/10.1016/j.epsl.2011.10.026

Harrison, T. N., Osinski, G. R., Tornabene, L. L., & Jones, E. (2015). Global documentation of gullies with the Mars Reconnaissance Orbiter Context Camera and implications for their formation. *Icarus, 252*, 236-254. doi:https://doi.org/10.1016/j.icarus.2015.01.022

Head, J. W., Mustard, J. F., Kreslavsky, M. A., Milliken, R. E., & Marchant, D. R. (2003). Recent ice ages on Mars. *Nature, 426*, 797. doi:10.1038/nature02114

ICPP. (2013, June 18, 2013). What is a GCM. Retrieved from http://www.ipcc-data.org/guidelines/pages/gcm_guide.html

Johnsson, A., Reiss, D., Hauber, E., Hiesinger, H., & Zanetti, M. (2014). Evidence for very recent melt-water and debris flow activity in gullies in a young mid-latitude crater on Mars. *Icarus, 235*, 37-54. doi:https://doi.org/10.1016/j.icarus.2014.03.005

Levy, J. (2012). Hydrological characteristics of recurrent slope lineae on Mars: Evidence for liquid flow through regolith and comparisons with Antarctic terrestrial analogs. *Icarus, 219*(1), 1-4. doi:https://doi.org/10.1016/j.icarus.2012.02.016

M. Dundas, C., S. McEwen, A., Diniega, S., J. Hansen, C., Byrne, S., & McElwaine, J. (2017). *The formation of gullies on Mars today*.

Malin, M. C., & Edgett, K. S. (2000). Evidence for Recent Groundwater Seepage and Surface Runoff on Mars. *Science, 288*(5475), 2330.

Mangold, N., Baratoux, D., Witasse, O., Encrenaz, T., & Sotin, C. (2016). Mars: a small terrestrial planet. *The Astronomy and Astrophysics Review, 24*(1), 15. doi:10.1007/s00159-016-0099-5

Martín-Torres, F. J., Zorzano, M.-P., Valentín-Serrano, P., Harri, A.-M., Genzer, M., Kemppinen, O., . . . Vaniman, D. (2015). Transient liquid water and water activity at Gale crater on Mars. *Nature Geoscience, 8*, 357. doi:10.1038/ngeo2412

https://www.nature.com/articles/ngeo2412#supplementary-information

Martínez, G. M., & Renno, N. O. (2013). Water and Brines on Mars: Current Evidence and Implications for MSL. *Space Science Reviews, 175*(1), 29-51. doi:10.1007/s11214-012-9956-3

McEwen, A. S., Dundas, C. M., Mattson, S. S., Toigo, A. D., Ojha, L., Wray, J. J., . . . Thomas, N. (2013). Recurring slope lineae in equatorial regions of Mars. *Nature Geoscience, 7*, 53. doi:10.1038/ngeo2014

https://www.nature.com/articles/ngeo2014#supplementary-information

McEwen, A. S., Eliason, E. M., Bergstrom, J. W., Bridges, N. T., Hansen, C. J., Delamere, W. A., . . . Weitz, C. M. (2007). Mars Reconnaissance Orbiter's High Resolution Imaging Science Experiment (HiRISE). *Journal of Geophysical Research: Planets, 112*(E5), n/a-n/a. doi:10.1029/2005JE002605

McEwen, A. S., Ojha, L., Dundas, C. M., Mattson, S. S., Byrne, S., Wray, J. J., . . . Gulick, V. C. (2011). Seasonal Flows on Warm Martian Slopes. *Science, 333*(6043), 740.

Millour, E., Forget, F., Spiga, A., Navarro, T., Madeleine, J.-B., Montabone, L., . . . Desjean, M. C. (2015). *The Mars Climate Database (MCD version 5.2)* (Vol. 10). ESPC.

Mustard, J. F., Cooper, C. D., & Rifkin, M. K. (2001). Evidence for recent climate change on Mars from the identification of youthful near-surface ground ice. *Nature, 412*, 411. doi:10.1038/35086515

Möhlmann, & Thomsen, K. (2011). Properties of cryobrines on Mars. *Icarus, 212*(1), 123-130. doi:https://doi.org/10.1016/j.icarus.2010.11.025

Möhlmann, D. T. F. (2011). Latitudinal distribution of temporary liquid cryobrines on Mars. *Icarus, 214*(1), 236-239. doi:https://doi.org/10.1016/j.icarus.2011.05.006

Ojha, L., McEwen, A., Dundas, C., Byrne, S., Mattson, S., Wray, J., . . . Schaefer, E. (2014). HiRISE observations of Recurring Slope Lineae (RSL) during southern summer on Mars. *Icarus, 231*, 365-376. doi:https://doi.org/10.1016/j.icarus.2013.12.021

Ojha, L., Wilhelm, M. B., Murchie, S. L., McEwen, A. S., Wray, J. J., Hanley, J., . . . Chojnacki, M. (2015). Spectral evidence for hydrated salts in recurring slope lineae on Mars. *Nature Geoscience, 8*, 829. doi:10.1038/ngeo2546

https://www.nature.com/articles/ngeo2546#supplementary-information

Ojha, L., Wray, J. J., Murchie, S. L., McEwen, A. S., Wolff, M. J., & Karunatillake, S. (2013). Spectral constraints on the formation mechanism of recurring slope lineae. *Geophysical Research Letters, 40*(21), 5621-5626. doi:10.1002/2013GL057893

Parker, T., Gorsline, D., Saunders, R., Pieri, D., & Schneeberger, D. (1993). Coastal geomorphology of the Martian northern plains. *Journal of Geophysical Research: Planets, 98*(E6), 11061-11078. doi:10.1029/93JE00618

Philip, G. M., & Watson, D. F. (1982). A PRECISE METHOD FOR DETERMINING CONTOURED SURFACES. *The APPEA Journal, 22*(1), 205-212.

Raack, J., Conway, S. J., Herny, C., Balme, M. R., Carpy, S., & Patel, M. R. (2017). Water induced sediment levitation enhances downslope transport on Mars. *Nature Communications, 8*(1), 1151. doi:10.1038/s41467-017-01213-z

Rodriguez, J. A. P., Fairén, A. G., Tanaka, K. L., Zarroca, M., Linares, R., Platz, T., . . . Glines, N. (2016). Tsunami waves extensively resurfaced the shorelines of an early Martian ocean. *Scientific Reports, 6*, 25106. doi:10.1038/srep25106

https://www.nature.com/articles/srep25106#supplementary-information

Smith, D. E., Zuber, M. T., Frey, H. V., Garvin, J. B., Head, J. W., Muhleman, d. O., . . . Sun, X. (2001). Mars Orbiter Laser Altimeter: Experiment summary after the first year of global mapping of Mars. *Journal of Geophysical Research: Planets, 106*(E10), 23689-23722. doi:10.1029/2000JE001364

Stillman, D. E., Michaels, T. I., Grimm, R. E., & Hanley, J. (2016). Observations and modeling of northern mid-latitude recurring slope lineae (RSL) suggest recharge by a present-day martian briny aquifer. *Icarus, 265*, 125-138. doi:https://doi.org/10.1016/j.icarus.2015.10.007

Stillman, D. E., Michaels, T. I., Grimm, R. E., & Harrison, K. P. (2014). New observations of martian southern mid-latitude recurring slope lineae (RSL) imply formation by freshwater subsurface flows. *Icarus, 233*, 328-341. doi:https://doi.org/10.1016/j.icarus.2014.01.017

U.S.G.S. (2014, December 16, 2014). Planetary GIS Web Server - PIGWAD. Retrieved from https://webgis.wr.usgs.gov/pigwad/maps/mars.htm

W.U. (2018, February 23, 2018). The Mars Orbital Data Explorer. Retrieved from http://ode.rsl.wustl.edu/mars/index.aspx

Watson, D. F., & Philip, G. M. (1985). A REFINEMENT OF INVERSE DISTANCE WEIGHTED INTERPOLATION *GEO-PROCESSING, 2*(4), 315-327.

8. Appendix

8.1 Extra Tables

Appendix Table 1: All the candidate sites with complementary coordinates. Note that this is not all the images that were surveyed. All in all 1569 images was examined were roughly 785 were unique images with coordinates.

Candidate sites	CENTER LATITUDE	CENTER LONGITUDE
ESP_039933_2145	34,078	306,258
ESP_033854_2335	53,346	289,007
ESP_034909_2300	49,902	288,38
ESP_035159_2295	48,993	303,905
ESP_035344_2260	45,718	293,698
ESP_035964_2265	45,935	288,712
ESP_044074_2285	47,996	288,258
ESP_034642_2195	39,153	21,255
ESP_037292_2175	37,212	33,26
ESP_043200_2220	41,81	25,069
ESP_043648_2255	45,065	38,202
ESP_046075_2200	40,351	24,246
ESP_046853_2200	40,16	22,972
ESP_047011_2240	43,217	28,472
ESP_048712_2225	42,24	23,312
ESP_049371_2175	37,204	32,867
ESP_050255_2195	38,9166	20,4276
ESP_023262_2310	50,681	26,449
ESP_017248_2170	36,87	59,671
PSP_009956_2160	35,715	56,48
ESP_046772_2085	28,287	75,425
ESP_044122_2335	52,973	57,466
ESP_034969_2135	33,023	93,444
ESP_016960_2265	45,969	0,189
ESP_018661_2265	45,926	0,061
ESP_024951_2200	39,411	356,588
ESP_025716_2200	39,648	350,488

Appendix Table 2: During the process of finding RSL, several other landforms were noted for potential future studies. In the table below it is possible to see which landforms were looked at and how many of them were discovered.

Landform	Number of landforms in researched images
RSL-feature	55
slope streaks	200
Dunes	712
Channels	158
Gullies	143
Spider	0
delta	1
dragon scale texture	4
stone stripes	6
small-scale lobes	51
veiki moraines	14
Talus	320
Fan	321
valley network	72
cracks	202
flow features (debris/grain)	663
dark streak	83
mesa	18
Ice	195
Teardrop feature	33
lobes	1
mounds	15
Knobbs and/or butte	6
Apron	13
Fretted terrain	16
Lineations	29

8.2 Ice surface cover images

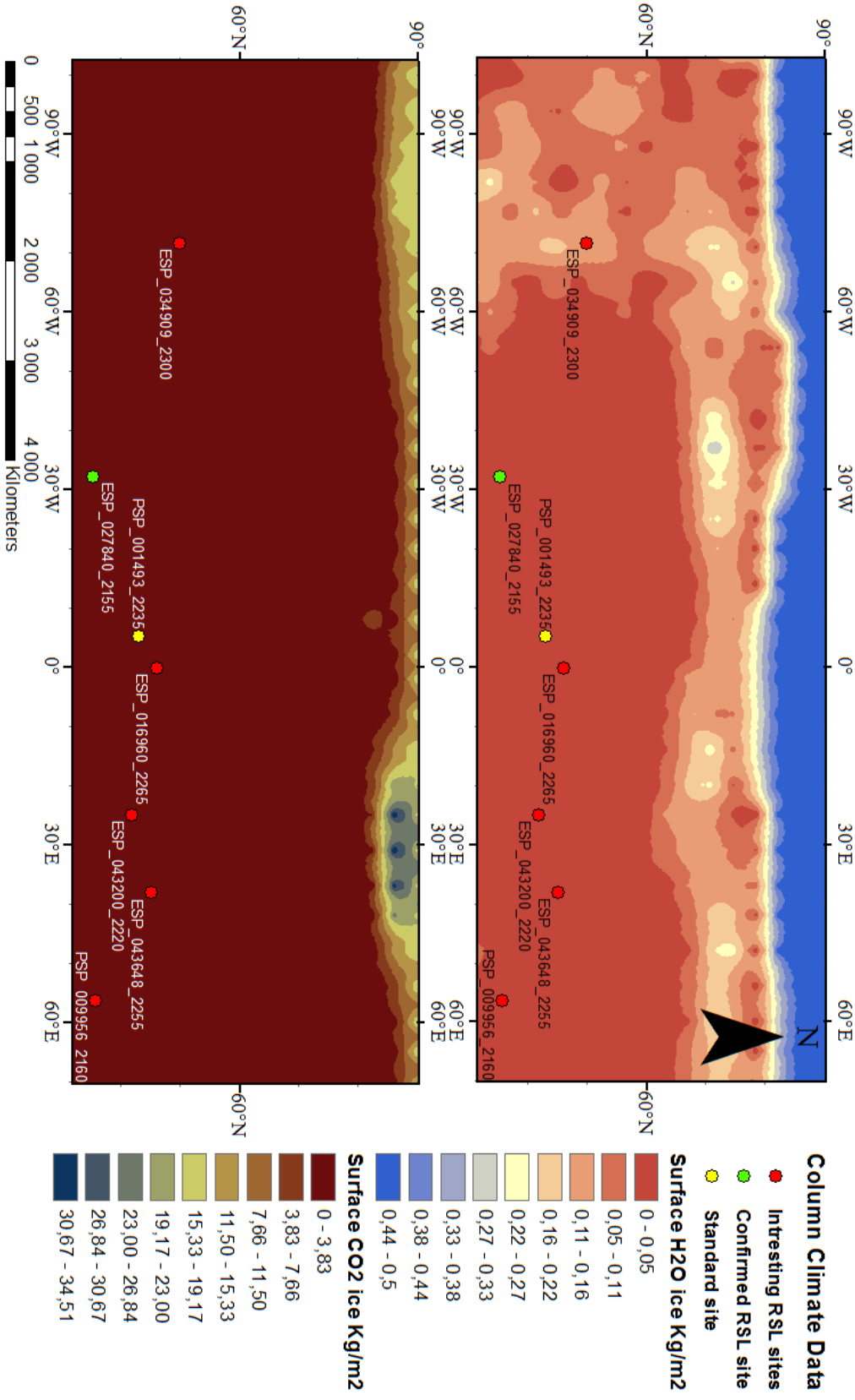

Appendix Figure 1: These images represent the ice cover on the northern hemisphere during the summer. The brighter map shows water ice while the darker map shows the CO_2 ice. Cartographer was Andreas Eriksson.

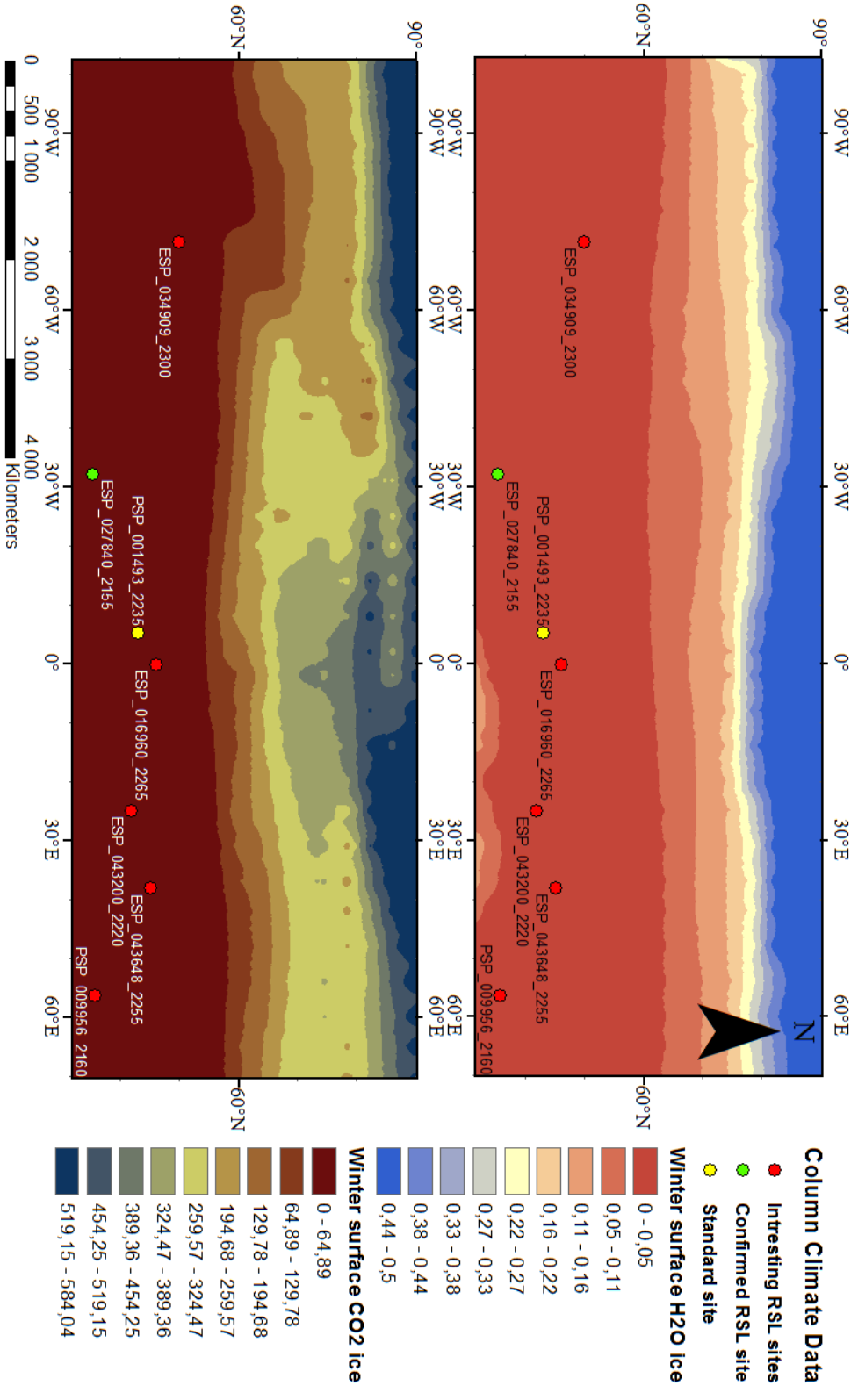

Appendix Figure 2: These images represent the ice cover on the northern hemisphere during the winter. The brighter map shows water ice while the darker map shows the CO_2 ice. Cartographer was Andreas Eriksson.

8.3 Hiview images of interesting sites

Appendix Figure 3: Hiview image of NE part of crater in ESP_034909_2300. The slope direction is SW. Solar incidence angle 43°, with the Sun about 47° above the horizon. Arrows in image point to potential RSL's. Credit: NASA/JPL/University of Arizona.

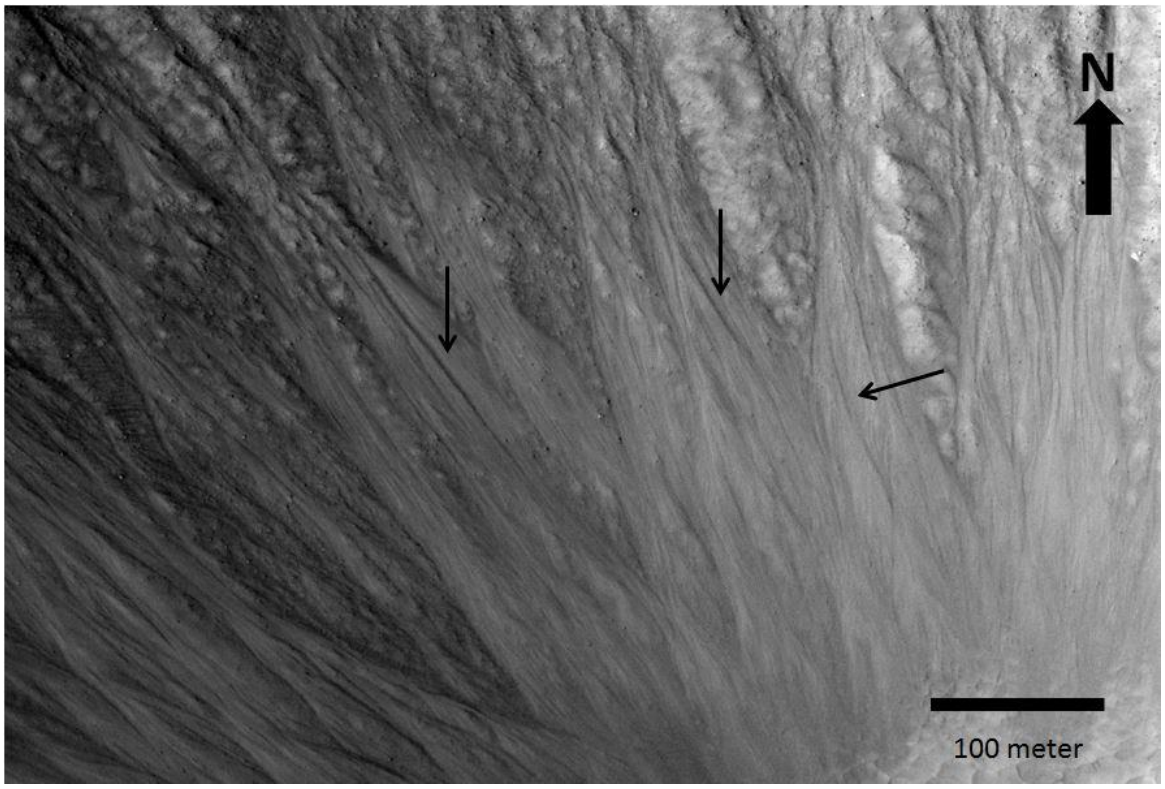

Appendix Figure 4: Hiview image of NW part of crater in ESP_034909_2300. The slope direction is SE. Solar incidence angle 43°, with the Sun about 47° above the horizon. Arrows in image point to potential RSL's. Credit: NASA/JPL/University of Arizona.

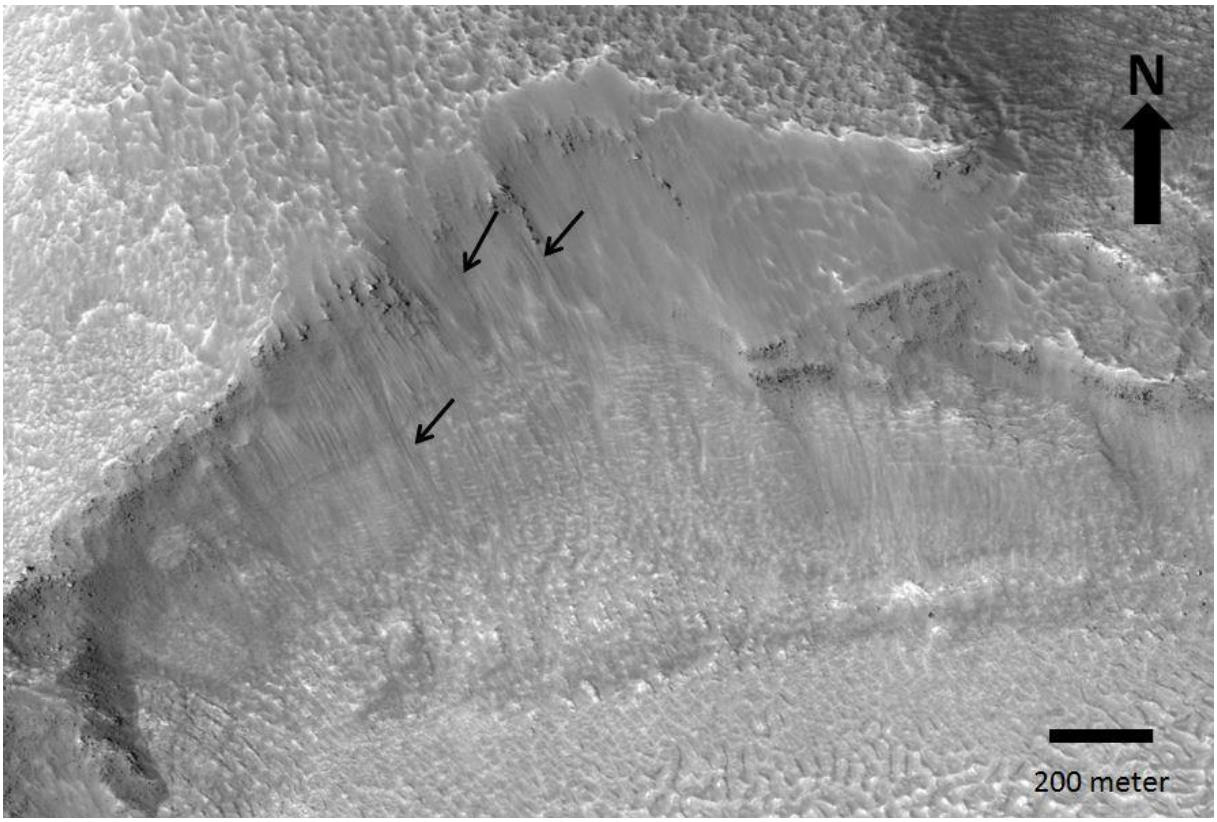

Appendix Figure 5: Hiview image of slope in ESP_043200_2220. The slope direction is S. Solar incidence angle 39°, with the Sun about 51° above the horizon. Arrows in image point to potential RSL's. Credit: NASA/JPL/University of Arizona.

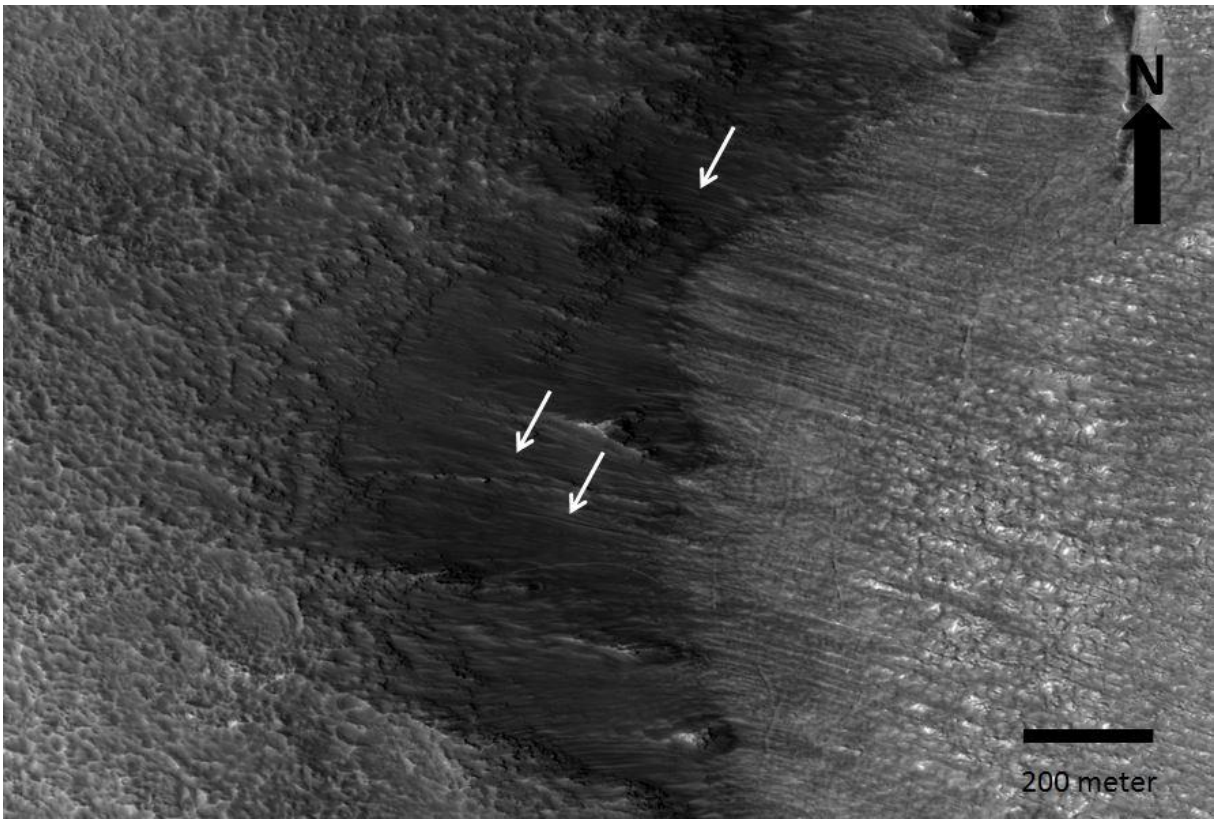

Appendix Figure 6: Hiview image of slope in ESP_043200_2220. The slope direction is E. Solar incidence angle 39°, with the Sun about 51° above the horizon. Arrows in image point to potential RSL's. Credit: NASA/JPL/University of Arizona.

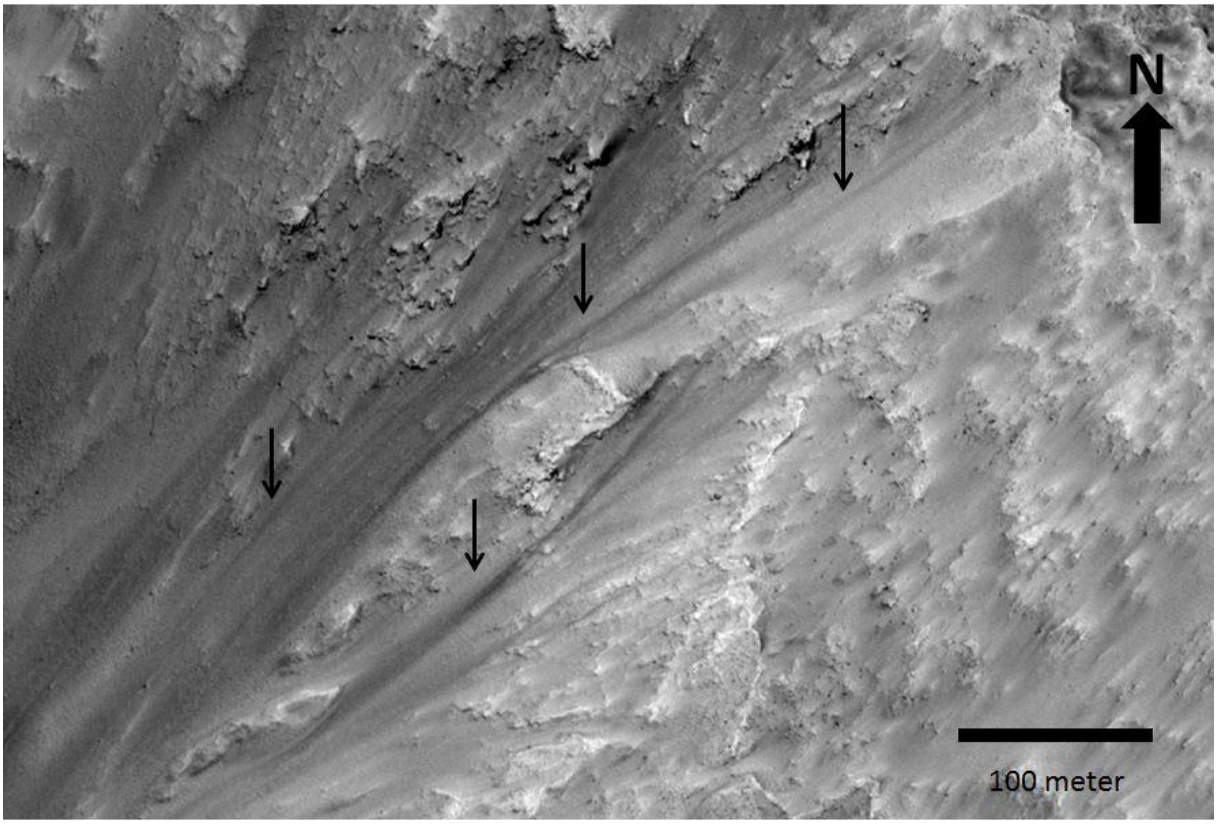

Appendix Figure 7: Hiview image of slope in ESP_043648_2255. The slope direction is SW. Solar incidence angle 41°, with the Sun about 49° above the horizon. Arrows in image point to potential RSL's. Credit: NASA/JPL/University of Arizona.

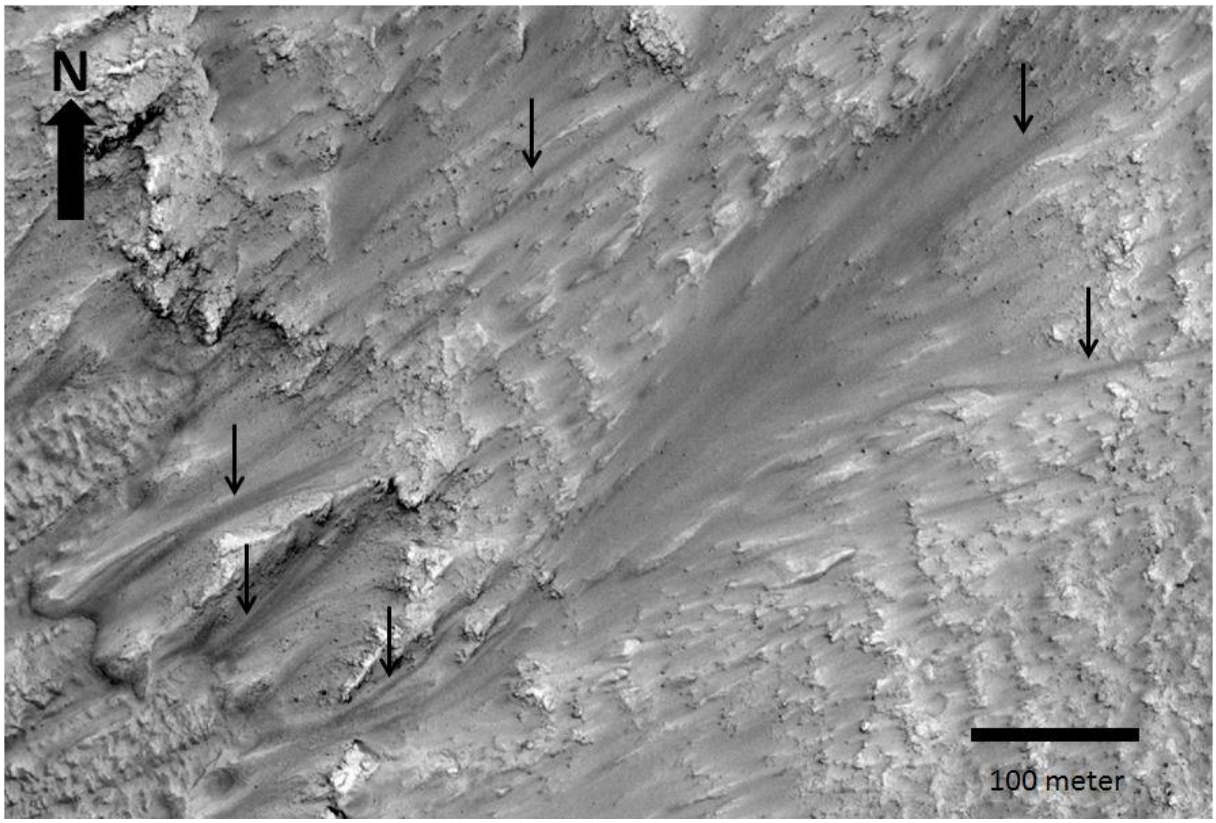

Appendix Figure 8: Hiview image of slope in ESP_043648_2255. Slope direction is SW. Solar incidence angle 41°, with the Sun about 49° above the horizon. Arrows in image point to potential RSL's. Credit: NASA/JPL/University of Arizona.

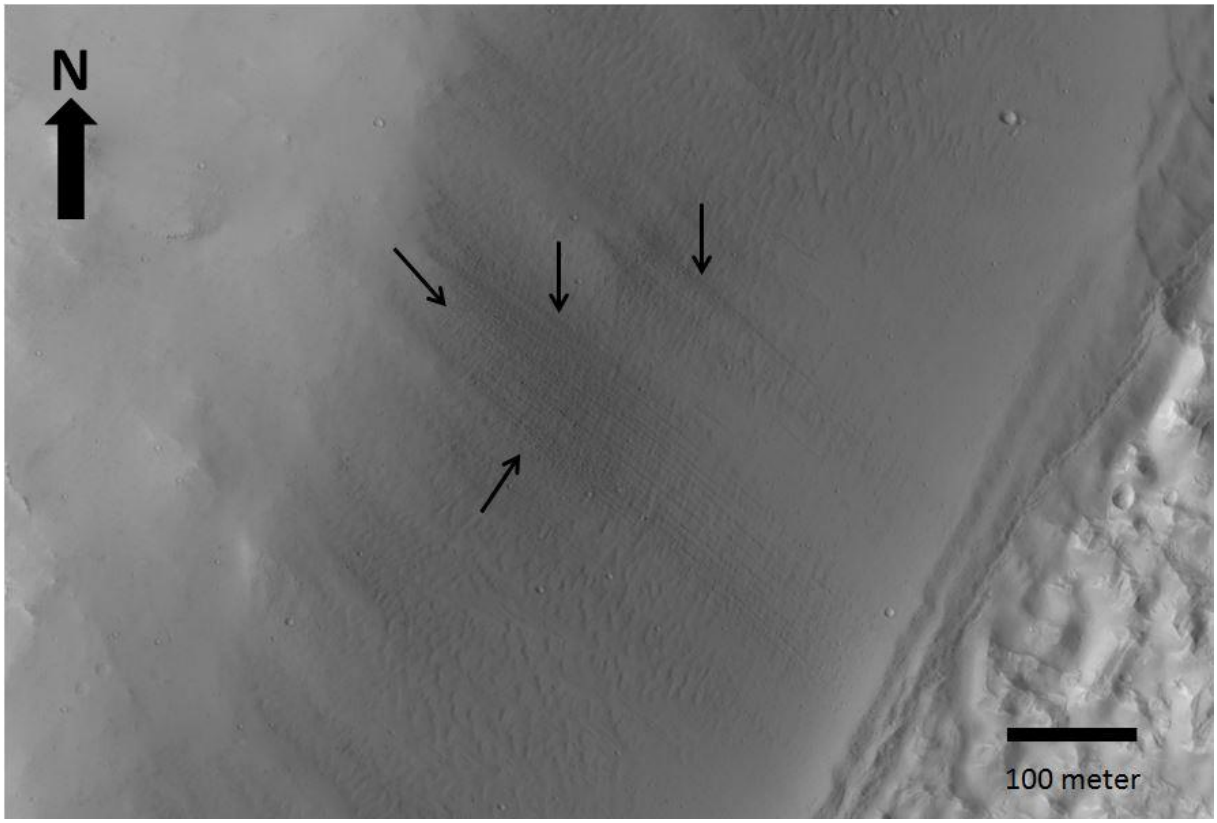

Appendix Figure 9: Hiview image of slope in PSP_009956_2160. Slope direction is SE. Solar incidence angle 45°, with the Sun about 45° above the horizon. Arrows in image point to potential RSL's. Credit: NASA/JPL/University of Arizona.

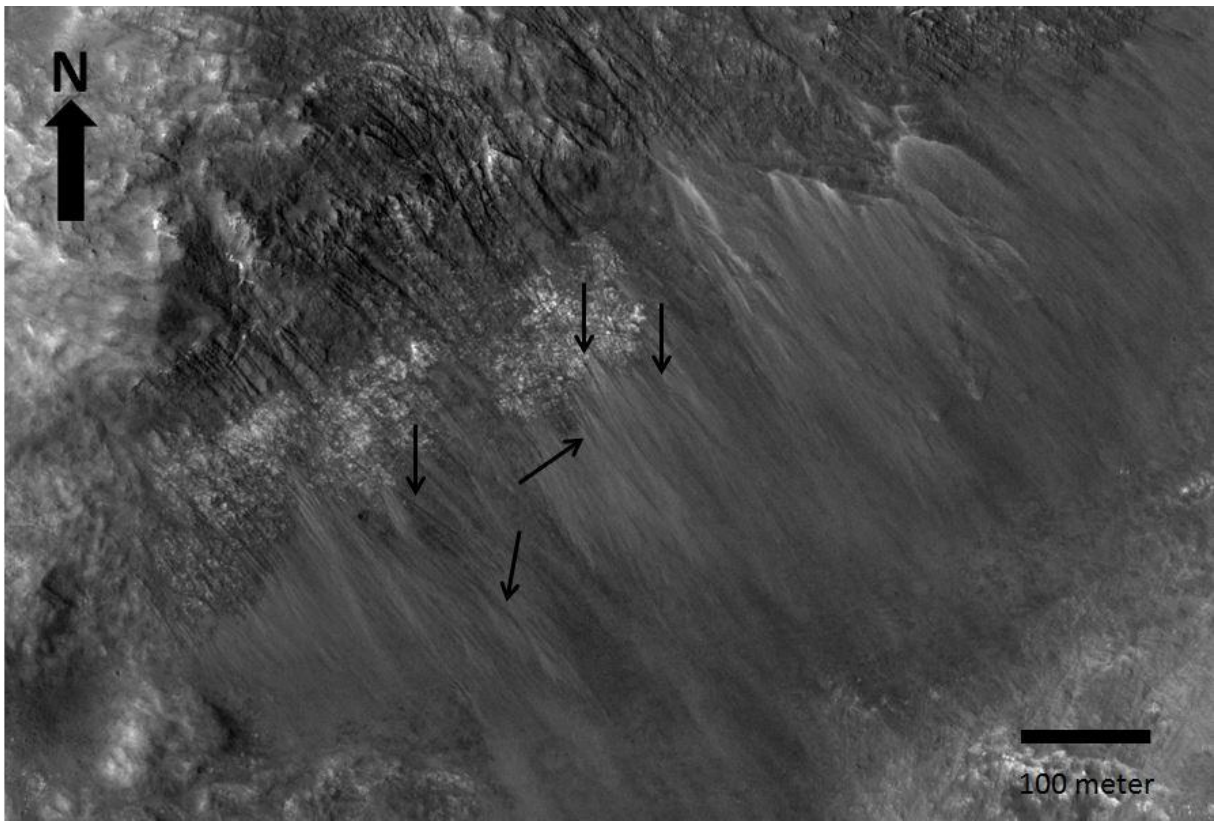

Appendix Figure 10: Hiview image of W slope in ESP_016960_2265. Slope direction is SE. Solar incidence angle 42°, with the Sun about 48° above the horizon. Arrows in image point to potential RSL's. Credit: NASA/JPL/University of Arizona.

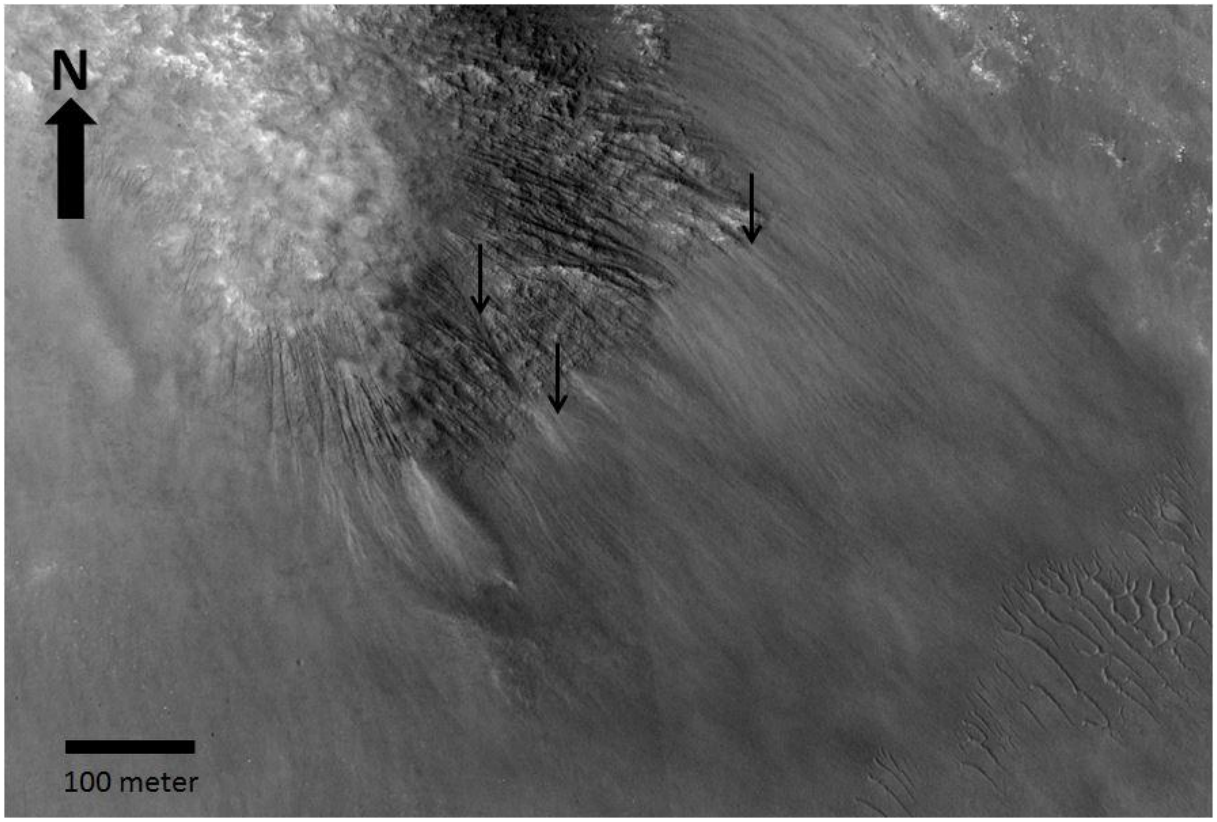

Appendix Figure 11: Hiview image of S slope in ESP_016960_2265. The slope direction is SE. Solar incidence angle 42°, with the Sun about 48° above the horizon. Arrows in image point to potential RSL's. Credit: NASA/JPL/University of Arizona.

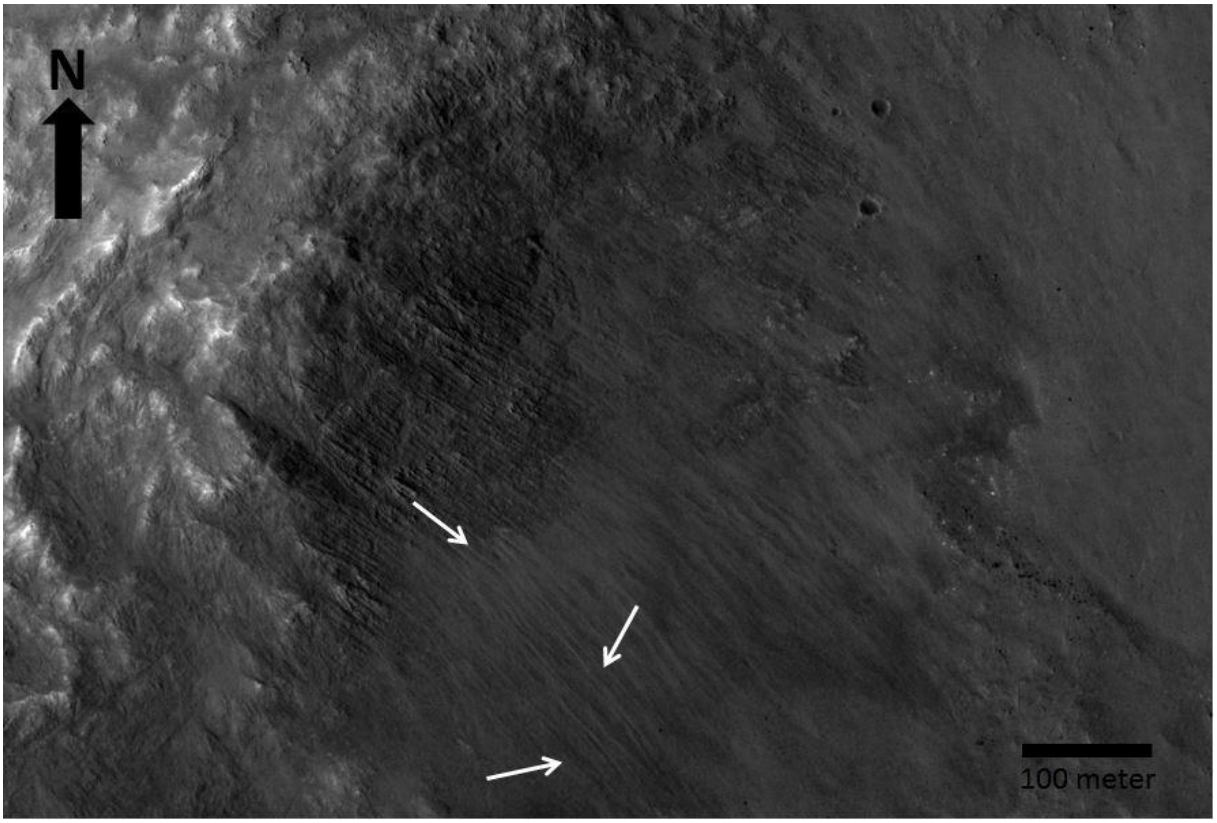

Appendix Figure 12: Hiview image of E slope in ESP_016960-2265. The slope direction is SE. Solar incidence angle 42°, with the Sun about 48° above the horizon. Arrows in image point to potential RSL's. Credit: NASA/JPL/University of Arizona.

Appendix Figure 13: Hiview image of the confirmed site in Acidalia Planitia. The image is ESP_027840_2155 and is from McEwen et al. (2013). The slope direction is W. Solar incidence angle 48°, with the Sun about 42° above the horizon. Arrows in image point to confirmed RSL's. Credit: NASA/JPL/University of Arizona.